Two-Dimensional Hydrodynamic Modelling of Flooding Using ASTER DEM in Ribb Catchment, Ethiopia

Tesfaye Haimanot Tarekegn
March, 2009

Course Title:	Geo-Information Science and Earth Observation for Environmental Modelling and Management
Level:	Master of Science (Msc)
Course Duration:	September 2007 - March 2009
Consortium partners:	University of Southampton (UK) Lund University (Sweden) University of Warsaw (Poland) International Institute for Geo-Information Science and Earth Observation (ITC) (The Netherlands)
GEM thesis number:	2007-17

Two Dimensional Hydrodynamic Modelling of Flooding Using ASTER DEM in Ribb Catchment, Ethiopia

by

Tesfaye Haimanot Tarekegn

Thesis submitted to the International Institute for Geo-information Science and Earth Observation in partial fulfilment of the requirements for the degree of Master of Science in Geo-information Science and Earth Observation for Environmental Modelling and Management

Thesis Assessment Board

Chairperson	Dr. Ir.C.M.M. Mannaerts (Associate Professor)
External Examiner	Prof. dr hab.K. Dąbrowska-Zielińkska
Internal Examiner	Dr. A.S.M. Gieske
Primary Supervisor	Dr.T.H.M. Rientjes
Second Supervisor	Dr. D. Alkema
Advisor	Alemseged T. Haile (Msc)

ITC International Institute for Geo-Information Science and Earth Observation
Enschede, The Netherlands

Disclaimer

This document describes work undertaken as part of a programme of study at the International Institute for Geo-information Science and Earth Observation. All views and opinions expressed therein remain the sole responsibility of the author, and do not necessarily represent those of the institute.

Abstract

The August 2006 flooding in Ribb Catchment in the Lake Tana Basin Ethiopia is one of the worst flooding events in recent years. This study focuses on studying the flooding characteristics in the floodplain of the catchment using two-dimensional (2D) hydrodynamic modelling and GIS techniques. In 2D flood modelling, both river and floodplain topography should be represented as accurately as possible. However, lack of topographic data at the required spatial resolution introduces a major limitation in the applicability of these approaches. The resolution of traditional data sources such as contour maps is too coarse to serve as an input for 2D flood modelling. As such, a Digital Elevation Model (DEM) that is generated from an ASTER image is used as a model input to represent the topography of the Ribb floodplain. A GIS procedure is developed to reconstruct the terrain properties of the main river reach as most of cross-sections from ASTER DEM largely deviated from field measured cross-sections. The study applied the 2D overland flow module of SOBEK 1D2D hydrodynamic flood model which is developed at WL/DELFT HYDRAULICS to study the flooding event of August 2006. The effect of interpolation on DEM accuracy and simulated flooding characteristics is also analysed. MODIS inundation maps and historic flood observations are applied to validate the model outputs.

The results of simulations show that 30.50 % of simulated flood extent for the August 14th flooding event explains MODIS flooding extent of the same event and 8 out of 12 historic flood observations match with simulated flood extent. The effect of interpolation resulted in 27.56% increase in flooding extent. The effect of Lake Tana water level is observed up to 13 km following the river. The percentage contribution of Lake Tana on the simulated flooding extent is some 8.55%.Some 67.64% of the inundation occurs in the area within a distance of some 6 km from the upstream boundary where flooding is mainly in the right bank of the river.

The results of this study show that ASTER DEM can potentially be used to estimate flooding characteristics in Ribb Catchment using SOBEK hydrodynamic flood model if proper GIS operations are applied. It also suggests that SOBEK is a powerful tool in predicting flooding characteristics of the Ribb floodplain. In addition, the study proves that geometric description of channel topography has significant effects on the outputs of hydrodynamic models. This study reveals that any change in the water level of Lake Tana affects the flooding pattern in the floodplain.

Key Words: Hydrodynamic Flood modelling, DEM, ASTER, SOBEK, MODIS, GIS

Acknowledgements

First of all I would like to thank God for helping me finish this work. My sincere gratefulness to my mother and my father and without them I wouldn't have succeeded in my study life.

I would like to thank the European Union for giving me a splendid opportunity to experience European culture and Education. I am also so thankful to all of my teachers in University of Southampton (UK), Lund University (Sweden) and University of Warsaw (Poland). I express my special gratitude to the course coordinator of the GEM programme Andre Kooiman for his follow up and support. I also like to thank Jorien Terlouw for her kindness and assistance throughout the course.

I offer my sincerest gratitude to my first supervisor Dr. Tom Rientjes who has supported me during my thesis work with his patience, effort and knowledge. I appreciate your help and comments to improve my writing skill. I further extend my cordial gratefulness to my second supervisor Dr. Dinand Alkema for his special support and encouragement since the start of my thesis. My heartfelt thanks to my advisor Alemseged Tamiru for his full passion and commitment to share his knowledge and past experience. I appreciate him for his encouragement throughout the thesis.

I would like to thank Mr. Surafel Mamo of Ethiopian Ministry of Water Resources and Gerard Reinink of ITC for providing me the required data for the thesis work.

My fellow classmates, you are so friendly and you deserve my genuine appreciation. I enjoyed pleasant time with you. Thank you so much all of you. I want express my appreciation to Tawanda for his honest support during my stay in Southampton.

Finally, I offer my greatest appreciation to Lens for her love and prayer.

Table of contents

List of figures

List of tables

1. Introduction

1.1. Background

The need to study the causes and effects of flooding has begun since flooding has become a problem to society when people and there valuables became affected. Historically, many solutions have been proposed to mitigate the effects of floodings but often knowledge on the actual cause-effect relation was lacking. With the advent of digital computers much emphasis has been on simulating and modelling of flood events and related characteristics and such is also the topic of this thesis work. The challenge here is to develop a reliable 2D flood model to simulate flood events for Ribb catchment.

Causes of flooding can be natural or human induced. Natural causes can be high and long lasting precipitation or extreme events such as earth quake and tsunamis. Man induced causes include failure of a dam or levee or, indirectly, urbanisation in flood prone areas. Mitigating on flood effects requires information on the flooding characteristics and how such characteristics propagate. Such information can be obtained through hydrodynamic models that are able to simulate flood extents, depths, levels, velocity and timing over a distributed model domain and over the time dimension. Hydrodynamic flood models solve governing flow equations that are based on the laws of mass, energy and momentum conservation. SOBEK is one of such model approach and is able to model flooding characteristics given that sufficient input data of good quality is available.

In hydrodynamic flood modelling, availability of data in the required spatial and temporal resolution is vital. Topographic data is one of such data used as an input in hydrodynamic modelling. Digital elevation models (DEM) are major sources of topographic data for representing floodplain and river topography however availability of the geometric data of river cross-sections is a major limitation. For such availability of a high resolution DEM is a prerequisite and as such for this study an ASTER DEM is selected. In absence of detailed surveyed cross section data, this DEM is used to construct river topography and related properties.

In order to test the model results, field data on flood inundation and flood levels are required. Data can be available through observed time series data or through image data that provide complete coverage of the inundation area. In this respect Horrit and Bates (2002) used SAR images to calibrate and validate simulated flood extent for River Seven in UK. Flood inundation maps produced by Dartmouth Flood Observatory (DFO) such as MODIS rapid response flood inundation maps are among these sources of data. Observed field data has been used by Werner (2004) who used 26 observations over the floodplain for the 1997 flood event in the towns of Utsi and Orilic in the Check Republic to test the performance of 1D2D SOBEK model.

In two-dimensional hydrodynamic flood modelling, river and floodplain topography are represented as a continuous surface. The representation of river and floodplain topography is through Digital elevation model (DEM) that in this work is by squared grid elements of equal size. In this study detailed data on river cross-sections or detailed bathymetric data to derive river topography as a continuous surface is not available and is considered a major limitation. Therefore river topography and related terrain properties have to be completed from a high resolution DEM using GIS techniques. Examples of similar applications in 2D hydrodynamic flood modelling can be found in Merwade et al.(2008) ; Merwade et al. (2005) and Tate et al (2002). Haile and Rientjes (2005) used a LIDAR DEM to derive river cross-sections for the purpose of 1D flood modelling by using the HEC-RAS hydraulic flow model . The river terrain is burned in the floodplain DEM to create a gridded surface of river and flood plain topography for 2D modelling.

In this research model results by the 2D hydrodynamic flood model called SOBEK for the August 2006 events are evaluated where ASTER DEM serves as input to represent flood plain topography. The flood model is applied to study jointly flood characteristics by river flows in Rib River and effects of Lake Tana water level. Flooding characteristics evaluated are flooding extent, depth, level and velocity that all are mapped. Results of simulated flood inundation extent are compared to MODIS flood inundation maps obtained from DFO. The simulated flood depths are also compared against historic flood depth observations.

1.2. Research Problems

In Ethiopia floodings are common in major river catchments owing to heavy summer rain and mountainous topography. In 2006 a total of 357,000 people were affected by that included some 136,528 people who had to abandon their homes (UNCHA, 2006).

The lower part of Ribb catchment is known as one of the flood prone areas by annual floodings in the Fogera floodplain. In, 2006 an extreme flooding affected and displaced 43127 and 8728 people respectively in the region (UNOCHA, 2006). Heavy rains fall for a number of days in the upstream part of the catchment caused the river to spill and to inundate the floodplain. Moreover by backwater effects from Lake Tana, the flooding was exacerbated.

Though flooding is frequently are observed in the floodplain, the flood management strategy has not gone beyond strengthening rescue and relief arrangements and other post flood measures which are totally devoid of any pre-flood management and planning strategy to minimize loss of life, property and environment (Assefa et al., 2008). Information regarding the flooding characteristics and its effect are essential for flood management bodies for decision making in flood management strategies such as construction of flood protection structures, to develop flood emergency plan and human settlement planning.

With advances in hydrodynamic flood modelling these days it is possible to model flood extent, depth, duration and even flood propagation in the temporal and spatial dimension. The limitation of the required topographic data for representing the topography of river and floodplain in the modelling is a major problem. Bates (2004) and Beven (1989) also describe the limitation of distributed data to parameterize and to validate distributed models. Topographic parameterisation in SOBEK is done by digital elevation models (DEM) and availability of DEM with spatial grid resolution that presumably could be effective is a major limitation. In 2D hydrodynamic flood modelling using SOBEK it is obvious that river channel bathymetry must be represented as a continuous surface but surveying river bathymetry and river cross sections to create a river terrain model is expensive. Details on bathymetry and cross-sections only partially can be extracted from public domain DEMs that information on real world features smaller than the grid element scale.

1.3. Research Objectives

From the background information and problem statement the following general and specific research objectives are formulated in this thesis work.

1.3.1. General Objective

To simulate flooding events in the Ribb catchment by using the two dimensional (2D) hydrodynamic flood model (SOBEK) and an ASTER DEM to represent the flood plain and river topography and related properties.

1.3.2. Specific Objectives

1. To construct a river terrain model from ASTER DEM
2. To study flooding characteristics of Ribb River
3. To determine the effect of Lake Tana water level on flooding characteristics.
4. To produce maps of flood depth, level and extent for the August 2006 flood events

1.4. Research Questions

The relevant research questions addressed in this research are:

1. How accurate can the observed inundated flood area be simulated by the selected model approach?
2. What is the effect of Lake water level on flood inundation extent?
3. How does the flood inundation pattern vary along the river?
4. What weight factor is most effective in IDW interpolation to create the river terrain model (RTM)?
5. Does effect of weight factor on the river terrain model have effect on simulated flood inundation extent?

1.5. Study Area

1.5.1. Location

Ribb catchment is one of the largest sub-catchment in the eastern part of Lake Tana basin, Ethiopia. This catchment is located between $11^0$43'N & $11^0$53'N latitude and $37^0$47' E &$37^0$54' E longitude. Ribb catchment has an area extent of 1586km^2. This catchment is drained by Ribb River which originates from Guna Mountain and finally joins Lake Tana in the vicinity where the river causes flooding. The

downstream part of the catchment is part of a wide flat floodplain (Fogera Floodplain) with a total area of 490km^2 adjacent to Lake Tana.

Lake Tana is the largest water mass of Ethiopia and it is the source of Blue Nile River. It has a total drainage area of approximately 15,000 km^2 and surface area of 3,060 km^2 at elevation 1786m above mean seal level (amsl). Lake Tana is located in the north-west highlands of Amhara Regional State, North Ethiopia at a latitude of $12^0$00'N, and longitude of $37^0$15'E.

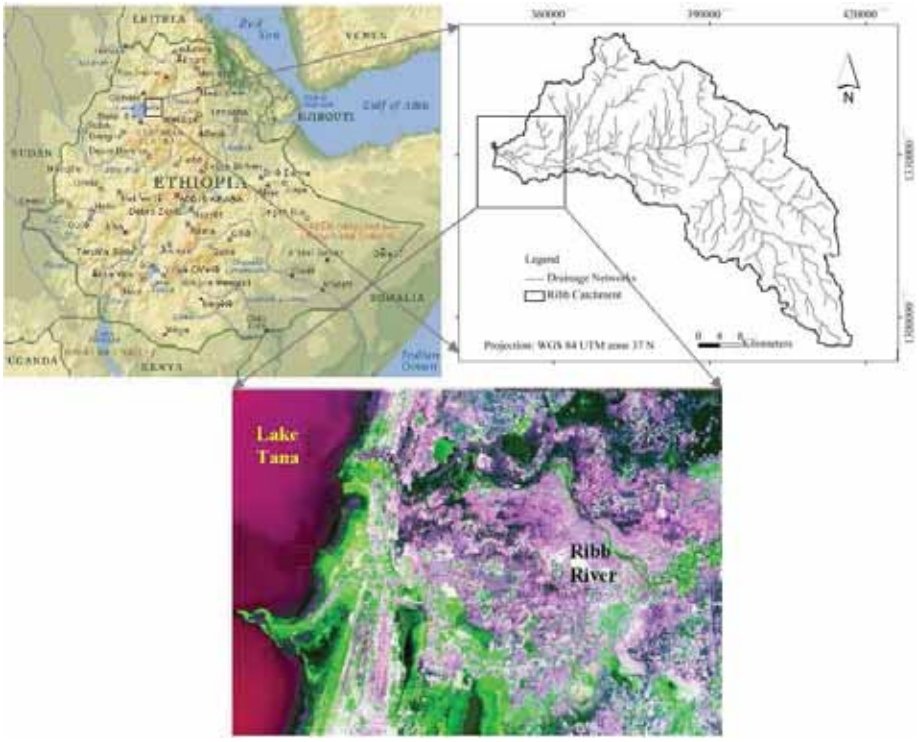

Figure 1-1: Location of the study area
(The lower picture is ASTER image acquired on 19/03/07)

1.5.2. Rainfall and flooding

Ribb catchment is characterised with a rainfall which amounts from 1100mm to 1530mm per annum. Ribb catchment experiences rainfall during the months June, July, August and September. The seasonal distribution of rainfall over the catchment is mono-modal; nearly 79% of the annual rainfall occurs from June to September.

Peak flows in the river occurs in August with peak average monthly flow of about 52m^3/s (Setegn et al., 2008). Figure 1-2 shows the average monthly distribution of rainfall (1964-2005).

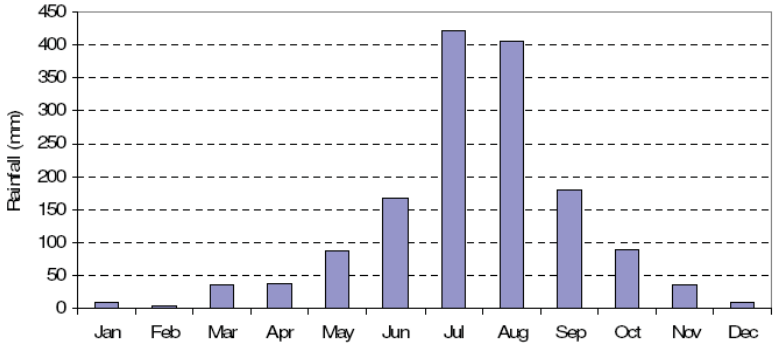

Figure 1-2 : Mean monthly rainfall of Ribb catchment

Flooding is a major problem in the downstream reaches of Ribb catchment and severe floorings of 1996, 1998, 1999, 2000, 2001,2003 and 2006 are among the most and severe events (Legesse and Gashaw, 2008). The river in its lower reach transgresses a flat plain which is vulnerable to flooding. The August 2006 flooding in the catchment was known for its long flood duration and devastation. Many people are forced to evacuate to other province for more than two months.

1.5.3. Topography and Land use

The elevation of the catchment ranges from a minimum of 1786m to 2150m amsl. The slope of the floodplain is 0.03% which is quite mild. The upstream of the catchment is highly mountainous while it is very flat at its lower reaches.

Land use of the flood plain is mainly dominated by cultivated lands. Figure 1-3 shows the distribution of land use classes. Most of the study area is characterized by cultivated lands as most of the area is rural.

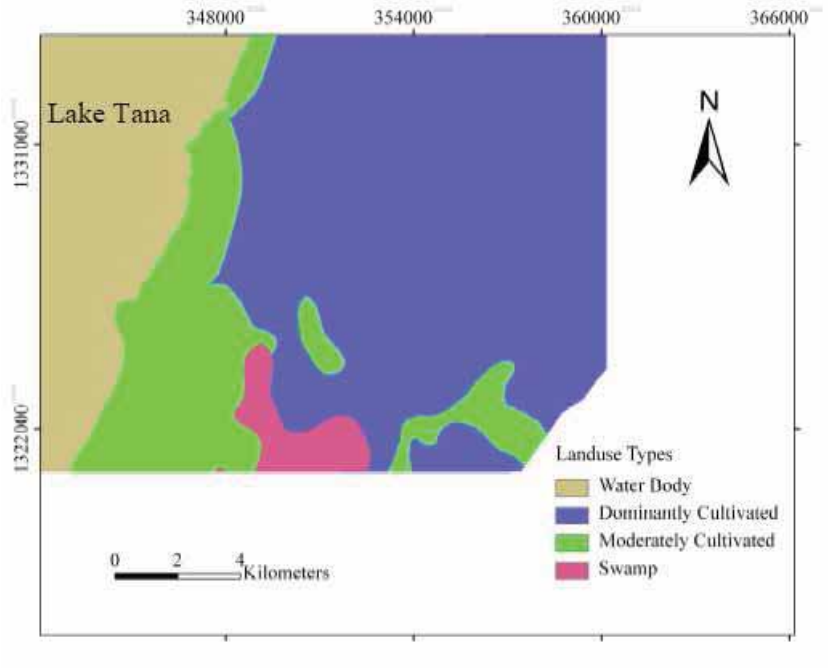

Figure 1-3: Land use map of the study area

2. Literature Review

2.1. Hydrodynamic Flood Modeling

2.1.1. General

The technology of capturing high-quality quantitative parameterisation data especially DEM and the development of efficient numerical and computational tools has brought big contribution for the development of flood models (Hunter et al., 2007). Flood models are a representation of the hydrologic and hydraulic processes in the river channel and flood plain. Accurate representations of the actual process is of paramount significance in predicting flood extent and depth, especially explaining the transient characteristics of river water flow in the model domain. Determining the variation of flow characteristics in spatial and temporal resolution enables to design flood evacuation plan quite efficiently (Haile and Rientjes, 2005).

2.1.2. Flood Modelling Approaches

Different modelling approaches are used in flood inundation modelling. The most common approaches include planar water surface approach, small and large cell approach, one-dimensional hydrodynamic models, two-dimensional hydrodynamic models and coupled one dimensional and two dimensional hydrodynamic models (Werner, 2004). The complexity of model approaches range from the very simple planar water surface approach in which the hydraulics of floodplain and main channel flow are ignored to the more advanced hydrodynamic models which are based on solving the hydrodynamic equations of flows.

In planar water surface approach a planar surface of water level observed at gauges is overlain on to a DEM and all areas below this surface are counted as flooded. As such, channel or floodplain routing is not applied. Large and small storage cell approaches are similar in their channel and floodplain routing both use uniform flow equations. The spatial discritisation in the former is that floodplain is discretised as inundation cells following existing natural boundaries while in the later floodplain discretisation are derived from the DEM.

Hydrodynamic models in general solve the Adhemar Jean Claude Barre De Saint Venant (1797-1886) equations of continuity and momentum developed in 1871 (Horritt and Bates, 2002). One dimensional (1D) model approach assumes flow is

transient only in longitudinal direction and water level is horizontal in transverse direction and solves the one dimensional flow governing equations at series of cross sections of the main river channel and the floodplain. The 1D approach is basically computationally efficient but it lacks simulation of transverse dynamics of flood wave, does not represent floodplain storage, topography is discretised as a cross section rather than a surface and the location and orientation of the cross section is defined subjectively (Hunter et al., 2007; Swan et al., 2007). One dimensional hydrodynamic flood models are commonly considered not sufficient to explain the physical and hydrodynamic conditions that are important to understand different river hydraulic processes (Merwade et al., 2008). Due to the previously mentioned limitations one dimensional model nowadays are being replaced by 2D and 1D2D hydrodynamic models.

Unlike the one dimensional, two dimensional model approaches consider variation of flow in longitudinal and transverse direction of the main river channel. It is very efficient to characterize flow in undefined and heterogeneous floodplains where the direction of flow is affected by other factors besides channel and floodplain slopes (Haile and Rientjes, 2005). 2D hydrodynamic models solve the full 2D shallow water equations. The development of 2D flood models is highly associated with the growth of efficient data acquisition technologies ad with the emergence of cheap and high speed computers. On the other hand 2D models need high resolution topographic data to represent the river channel cross section and the availability of these data is scarce. Purely 2D hydrodynamic models are also computationally time intensive. Werner (2001) explains that “using a two-dimensional flow model based on the topography has the drawback that computational requirements are high”. In order to address the problems associated with 1D and 2D models, the combined 1D2D models are developed in such a way that 1D represents the channel flow and river structures (culverts, drains, bridges) and the 2D represents the floodplain and effects of existing infrastructures (buildings and roads) in the flood plain (Haile and Rientjes, 2005; Swan et al., 2007). These models perform better for a condition where channel width is narrower than the grid size of 2D domain. The most widely used flood models are described in section 2.4.

Even though all modelling approaches have their own specific limitations a wide range of applications to real world problems are known. For instance 1D hydrodynamic flood models are less suited to a condition where floodplain flow is complex but they are better suited to a condition where there is a single dominant flow direction such as valley flooding.

2.1.3. Solution Approaches to Hydrodynamic Models

Flow governing equations used in hydrodynamic models are a complex set of continuous differential equations. The differential equations developed by St. Venant and described in equation 3-1,3-2 and 3-3 are such flow governing equations that are applied in two dimensional hydrodynamic flood modelling. Solving these equations through analytical methods is not possible (Dyhouse et al., 2003). They are solved through a numerical method which solves continuously varying (in time and space) differential terms at discrete points in space and discrete moments in time. The solution is obtained at a number of discrete points (distance interval, Δx) and a number of discrete times (Δt) for which derivatives are approximated by their finite difference. The numerical solutions involve conversion of the continuous differential equation in to a system of discrete algebraic equations which are solved through iteration and this gives an approximate solution.

There are different approaches used in descritisation i.e. to convert the continuous differential equations (continuous solution domain) in to a discrete system of algebraic equations (discrete solution domain). The most common methods include finite difference approaches, finite element approaches and finite volume approaches. In these approaches the continuous real world space and time dimensions are replaced by discrete finite increments to give an approximate of the differential equations or its solution. The use of either of the approaches depends on the problem under consideration. In SOBEK the two dimensional continuity and momentum equations are solved by finite difference approach (Dhondia and Stelling, 2002; Stelling and Duinmeijer, 2003).

2.1.4. Initial and Boundary Conditions

While applying flood model to a certain catchment, the model parameters, the initial (model) condition and boundary conditions have to be specified. Boundary conditions serve to introduce the influence of the external forces to the model domain such as river inflows and lake levels. The initial condition is the hydraulic state (water level or flux) in the model domain as defined prior to the actual simulation. Initial conditions can be defined based on information on gauges or through introducing a so-called warm-up that precedes the actual simulation period. In flood modelling also the upstream boundary and downstream boundary conditions has to be defined prior to the simulation. Boundary conditions are generally specified from hydrometric data such as time series data of discharge and stage or simulated discharge hydrograph. Mathematically, there are three types of boundary

conditions: Specified head boundary (Dirichlet Condition), Specified flow boundary (Neumann Condition) and mixed boundary condition or head-dependent flow boundary (Cauchy Condition).

2.1.5. Topographic Representations

In flood modelling floodplain DEM and surface roughness are very important model inputs. The outputs from hydrodynamic models such as flow depth, velocity and flood extent depends on the values of inputs from DEM as flow governing factors such as slope, flow direction and inundation area are affected by DEM resolution. Model outputs for different DEM resolutions are different due to the fact that the grid resolution has significant influence in representing the topography. Selecting the appropriate DEM resolution in flood modelling is very important for two reasons: to accurately represent the floodplain and channel topography and to consider the simulation time. The finer the DEM grid resolution, the longer the simulation time becomes while a coarser DEM resolution leads to longer simulation times. At courser resolutions also details on roads and buildings are lost since spatial scales of such properties fall within the scale of the selected grid element of the DEM.. It is very important to represent topography as accurately as possible as outputs of hydrodynamic flood models mainly depends on the accurate parameterisation of the topography. In 2D hydrodynamic flood modelling selection of an appropriate DEM resolution is vital to achieve optimal calculation time, however, the effect of using low resolution DEM is that predictive capability of the model reduces. More details about issues of grid size and computational time are explained by Werner (2001) and Haile and Rientjes (2005). In two dimensional hydrodynamic flood modelling it is very important to represent the geometric information of river channel and the flood plain as a continuous surface. The limitation of one dimensional models to represent the actual physical and hydrodynamic river processes forces one to use 2D models (Merwade et al., 2008). Parameterization of topography in 2D models is made by using DEMs which represents both floodplain and river channel topography. River topography, however, is usually not well represented in low resolution DEM. For better representation of the hydraulic processes in the river, a river terrain model can be developed and then burned in to floodplain DEM using GIS techniques and the resulting DEM is used as input to 2D modelling (Merwade et al., 2008)..

2.1.6. Surface Roughness

The main calibration parameters in flood modelling are roughness values of the floodplain and the main channel. A value for this parameter is assigned based on the land cover or land use type of the flood plain and the type of bed material in the main channel and its alignment. Manning roughness values for different surface materials and channel alignment are indicated in Arcement and Schneider (1989) and Chow (1959). Manning's n and Chezy C roughness values are widely applicable for roughness parameterisation in flood modelling (Werner, 2004). In two dimensional modelling surface roughnesses should be parameterised in the same resolution as the DEM (topography). In SOBEK roughness values for each grid cell of the DEM are assigned as constant value for all or as spatially variable value which are defined in a separate layer of roughness values. The grid size and extent of roughness layer should be same as the DEM.

2.2. ASTER Topographic Data

2.2.1. General

Digital elevation models are crucial for analysis of topography and modelling of surface processes typically in distributed models. Hydrodynamic flood modelling tools such as SOBEK require a DEM as an input for topographic parameterisation. Advanced Space Borne Thermal Emission and Reflection Radiometer (ASTER) which is onboard the National Aeronautics and Space Administration's (NASA's) Terra satellite is one of the sources of DEM. The ASTER sensor has been acquiring topographic data in operational mode since March 2000 (Hirano et al., 2003).

2.2.2. Data Acquisition

The ASTER system is equipped with 14 nadir looking spectral bands ranging from visible, near infra red and short wave infra red to thermal infrared spectral bands in addition to a backward looking VNIR band. The bands which are used to acquire a topographic data are the VNIR (Visible and near Infra Red) bands which have a spatial resolution of 15m. The nadir viewing band is called 3N and backward looking band is 3B (Figure 2-1). Two successive images of the same area are acquired with a time interval of approximately 55seconds by each sensor at different viewing angles resulting in stereo pairs of images which are subsequently used to measure height of the topography. These stereo image data are recorded only in Band 3 (NIR, 0.78 to 0.86μm) using both nadir and aft-looking telescopes. ASTER

along-track stereo mapping capability makes unique in such a way that the effect of climatic conditions between data acquisition is reduced and uniform environment is maintained unlike SPOT and ERS radar interferometery which complete the stereo pairs while revisiting (Stevens et al., 2004).

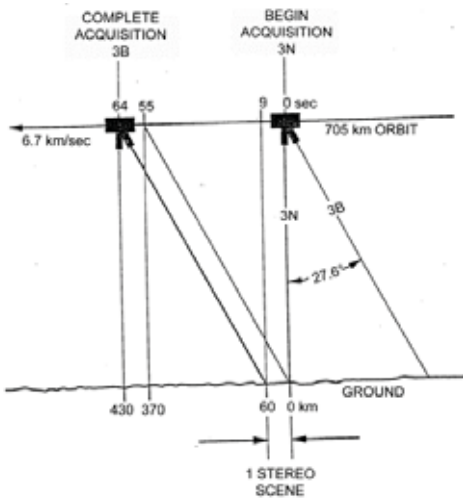

Figure 2-1: Imaging orientation and data acquisition timing for ASTER.

The stereo pairs are used to generate two types of DEM: relative DEM which is generated by automatic stereo correlation without the use of ground control points(GCPs) and absolute DEM which is generated by using GCPs in which the elevations are referenced with respect to sea level (Fujisada et al., 2001) . The accuracy of relative DEM ranges from +/-10 to 30m and that of absolute DEM ranges from +/- 7 to 50m depending on the number of GCPs (Hirano et al., 2003). According to a study by Cuartero et al. (2004) TERRA-ASTER images are able to generate a DEM with a root mean square error (RMSE) (see Equation. 3-4) that is smaller than the pixel size of the DEM.

2.3. Model Calibration, Sensitivity Analysis and Validation

There is always a need to analyse the difference between the values of a model output with observed values under the same time frame. It is not likely to find simulated values that do not deviate from observed, so it is essential to bring the difference to an acceptable and reasonable limit. This can be done by a process called model calibration that is a procedure of adjusting model inputs to match the model output with measured/observed data for the selected period and situation

entered to the model. The result of model calibration can be tested by accuracy criteria such as Nash-Sutcliffe model efficiency parameter and RMSE. In flood modelling the most important calibration parameter is the roughness coefficient. It is important to know which parameter or model input has high influence on the model output. This process of analysing the influence of each input or parameter by changing the value of one or more of them at a time is usually termed as sensitivity analysis. In flood modelling, hydrodynamic models are sensitive to physical model parameters (DEM resolution and surface roughness), initial and boundary conditions. Also a model has to be checked for its accuracy and predictive capability that is by calibration and validation. "A model is said to be validated if its accuracy and predictive capability in the validation period have been proven to lie within acceptable limits or errors for a particular practical purpose.'' Hunter et al.(2007). In flood modelling data for calibration and validation include flood inundation data (satellite imagery or flood inundation maps), field observations (distributed flood depth observations), and hydrometric data (gauged river stage or flow).

2.4. Model Selection

Selecting potentially an appropriate modelling tool in any research. There are various criteria which can be applied for choosing the most suitable model. According to Cunderlik and Simonovic (2003) the choice mainly depends on the requirements and needs of the research or project under interest. Cunderlik and Simonovic(2003) put the following as criteria.

1. Required outputs of the model
2. Availability of input data
3. Prices and availability of the model and
4. The model structure

There are different flood modelling tools which have their own distinct model structure and solution procedures. Most widely used one dimensional flood modelling tools include HEC-RAS, FLDWAV, ISIS, FLUCOMP and MIKE11.Two dimensional flooding models include MIKE21,DELFT-FLS,DELFT 3D, RMA2 and TELEMAC-2D and integrated one and two dimensional models include MIKEFLOOD, SOBEK and LISFLOOD-FP. Nowadays most flood inundation modelling projects prefer applying the 1D2D flood models(Dhondia and Stelling, 2002; Swan et al., 2007). In this research the SOBEK flood model is applied for its availability and its computational capability. SOBEK is able to simulate complex

flows and water related processes in almost any system (Dhondia and Stelling, 2002).

2.5. Remote sensing and GIS in hydrodynamic flood modeling

There are enormous difficulties to collect data in the required spatial and temporal coverage through field work. Moreover, the spatial and temporal coverage of ground data collection is very limited. Developments in remote sensing have solved most such difficulties. Spatially distributed data for topography parameterization, friction parameterization and model validation are very essential in flood inundation models. Remote sensing along with GIS nowadays is playing vital role in development of flood modelling. "Whilst there is a long way to go before we can claim a true distributed capability in flood inundation modelling, it is possible to argue that remotely sensed data has allowed a significant breakthrough to be made." Bates (2004).

Remote sensing nowadays is an invaluable source of information in flood modelling. Most of data inputs to flood model is directly or indirectly extracted from remotely sensed data. Some of important data used in flood modelling that are obtained from remote sensing include DEM (river and floodplain topography), land cover map and flood inundation maps.

Remote sensing also is used in validation and calibration of flood models. In flood extent mapping both optical and radar remote sensing can be used. Earth observation missions such as moderate resolution imaging spectrometer (MODIS),Environmenta l Satellite (ENVISAT), Earth Resource Satellite (ERS), RADARSAT, Landsat, Satellite Pour l'Observation de la Terre (SPOT), and Advanced Very High Resolution Radiometer (AVHRR) are used in flood extent mapping (Smith, 1997). Airborne and satellite Synthetic Aperture Radar with its capability to observe flooding event day or night, in any atmospheric condition is a major source of satellite image for the purpose of mapping flood extent and to be used in calibration /validation of flood models. In this respect Horritt and Bates (2002) applied RADARSAT and ERS satellite SAR images which are acquired in C-band are used to calibrate and validate simulated flood extent for River Seven in UK. Dartmouth Flood Observatory (DFO) also supplies archives of flood inundation maps produced using remote sensing to detect, measure, and map river discharge and river flooding, world-wide. Such source of inundation maps solves the limitation of availability of satellite imagery acquired on a particular flooding event. In this study as such data MODIS rapid response inundation map is used for validation of model results.

Moreover, topographic data such as ASTER DEM and Airborne light detection and ranging (LiDAR) DEM are acquired through remote sensing.

Since the attempt to couple GIS with hydraulic models started in 1975 (Nunes Correia et al., 1998), GIS has helped in handling and processing of spatial data. The development in integrating remote sensing with GIS has improved the growth in flood modelling. Most distributed models are capable of predicting flood spatially and temporally owing to the strong integration of these models with GIS for sharing spatial data. GIS techniques are important for both pre-processing and post processing of model inputs and outputs. In 2D hydrodynamic flood modelling river terrains models are developed by GIS techniques (Merwade et al., 2008; Merwade et al., 2005; Tate et al., 2002). The GIS techniques include interpolation of surveyed cross-sections, interpolation of discrete bathymetry points, and integration of surrounding topography with surveyed cross-sections and/or bathymetry points. Studies by Merwade et al.(2008) ; Merwade et al. (2005) and Tate et al.(2002) explain the possibility of creating river terrains or geospatial representation of river channels from cross sections through GIS techniques. Tate et al.(2002) also presented a GIS technique to import cross section data created in HEC-RAS to be used as a source of river bathymetry and then the cross sections are interpolated to create continuous river channel surface. Merwade et al. (2006) describes different spatial interpolation methods used while interpolating river bathymetry and explains the accuracy, the simplicity and computational effectiveness of inverse distance weighting (IDW) method of interpolation. Haile and Rientjes (2005) extracted cross-sections from LIDAR DEM for the purpose of 1D flood modelling by using 1D flood model called HEC-RAS. Figure 2-2 shows how GIS data and flood modelling are integrated

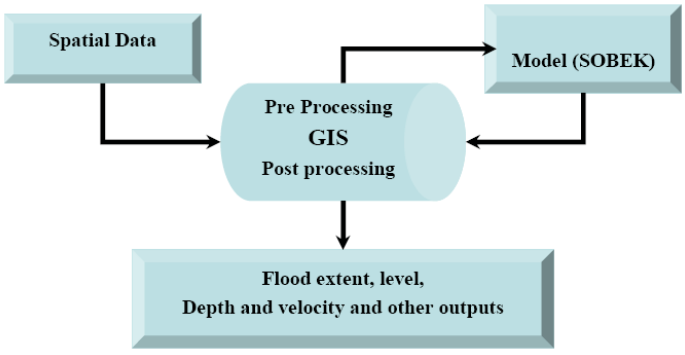

Figure 2-2: The integration of GIS and flood modelling

2.6. Previous Studies on Ribb Catchment

Though flooding is a common problem in the floodplain of the Ribb catchment researches regarding this are limited. The current flood problems and the lack of studies in the area show the importance of an in-depth study. Research by Assefa et al. (2008) is on developing flood forecasting and early warning decision tool for Fogera Floodplain based on rainfall forecasts and hydrological model. It mainly focuses on a quantitative precipitation forecast based flood forecasting model using HEC-HMS rainfall-runoff model for supporting flood early warning decision making. They set thresholds for the discharges in the river and comparison is made among the forecasted flow and the threshold to issue warning. The other research which is done by Legesse and Gashaw (2008) is on developing a map of flood hazard and risk levels for Fogera Wereda which is located in the flood plain of the Ribb-Gumera catchment. Moreover, they explained that land cover change (degradation of the land cover) in the upstream of the two catchments is contributing to flooding. They used a simple planar water surface approach for mapping the flood extent which is actually less realistic from flood modelling point of view.

3. Materials and Methods

3.1. Model Approach

Governing Flow Equations

SOBEK 1D2D hydrodynamic flood model is developed at WL/DELFT HYDRAULICS and allows for one dimensional (1D) channel flow and two dimensional (2D) overland flow modeling. In SOBEK water flow characteristics are computed by solving the so-called full Saint Venant differential equations. The model domain is spatially discretised into staggered rectangular grids (Stelling and Duinmeijer, 2003) to represent floodplain and river topography. SOBEK 2D module is able to handle overland flow with extensive detail incorporating structures like roads, railways, dykes etc. The 1D2D coupled module of SOBEK is particularly suitable for conditions where a channel width is smaller than the size of 2D grid cells of the DEM.

In SOBEK, 2D shallow water equations are solved to simulate overland flows based on the law of conservation of mass and momentum. These are described as continuity equation (3-1), momentum equation for x-direction (3-2) and momentum equation for y-direction (3-3) as described in SOBEK online help (www.sobek.nl).

$$\frac{\partial \xi}{\partial t} + \frac{\partial (uh)}{\partial x} + \frac{\partial (vh)}{\partial x} = 0 \qquad 3\text{-}1$$

$$\frac{\partial u}{\partial t} + u\frac{\partial u}{\partial x} + v\frac{\partial u}{\partial y} + g\frac{\partial \xi}{\partial x} + g\frac{u|V|}{C^2 h} + au|u| = 0 \qquad 3\text{-}2$$

$$\frac{\partial v}{\partial t} + u\frac{\partial v}{\partial x} + v\frac{\partial v}{\partial y} + g\frac{\partial \xi}{\partial y} + g\frac{u|V|}{C^2 h} + av|v| = 0 \qquad 3\text{-}3$$

where: ζ water level above plane of reference(m)

u flow velocity in x-direction (ms^{-1})

v flow velocity in the x-direction(ms^{-1})

C Chezy coefficient ($\sqrt{m/s}$)

V velocity: V= $\sqrt{u^2 + v^2}$

h total water depth: ζ+d (m)

d depth below plane of reference (m)
a wall friction coefficient(m^{-1})

The simplified forms and solution procedures of equation 3-1,3-2 and 3-3 are briefly described in Dhondia and Stelling (2002) and Stelling and Duinmeijer (2003).

In this work the 2D module of SOBEK is selected since the grid size of the applied ASTER DEM is smaller than the actual river width (see also Haile and Rientjes (2005)).

3.2. Model Setup

3.2.1. Boundary and Initial Conditions

Upstream Boundary Condition

For simulation of the upstream boundary condition twice daily observations are available from the Ethiopian Ministry of Water Resources (EMoWR). The data is collected at a gauging station which is located near Addis Zemen at 12^0 00' N and 37^0 43' E at an elevation of 1795 m amsl. The data that serves as a boundary condition is the flow discharge that was observed for the period August 1st to 16th for the year 2006. This period has been selected since flooding is severe with various peak flows and since satellite based inundation maps by MODIS are available. The solid lines in Figure 3-2 show the upstream boundary condition (BC) that was specified for the so called warm-up period, the first simulation and the second simulation period. This boundary condition is a specified flow boundary that commonly is referred to as Neumann boundary condition. The figure shows that river flow pattern is highly variable and starts to drop after August 19th.

Figure 3-1 : Ribb Gauging Station at Addis Zemen

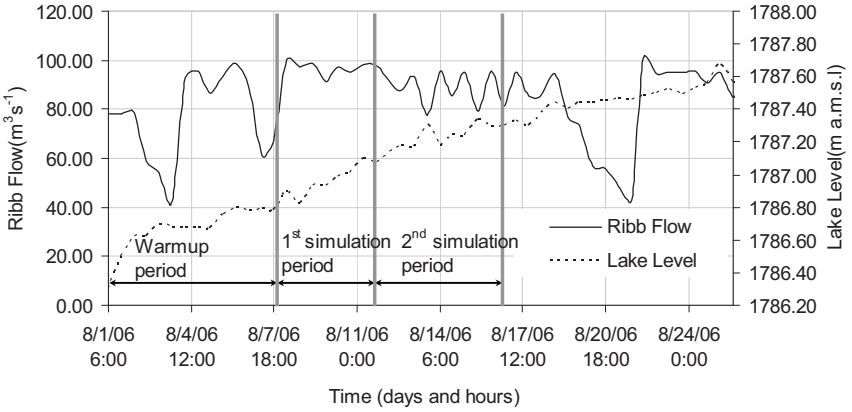

Figure 3-2: Ribb flow representing the upstream boundary and the Lake level representing the downstream boundary.

Downstream Boundary Condition

The downstream boundary condition is the water level of Lake Tana that is collected twice a day at a gauge located in Bahir Dar at $11^0$35' N and $37^0$22' E. The zero level of this staff gauge corresponds to a level of 1783.52 m amsl for the period before 2003 and 1784.52 m afterwards. In SMEC (2007) it is reported that the lake level data seems to be of acceptable quality though there is a maximum of 3 to 5 cm wind effect on the daily level variation. The broken line in Figure 3-2 shows the

downstream boundary condition that was specified for the warm-up period, the first simulation and second simulation period. As such the downstream boundary is a specified head boundary condition that commonly is referred to as a Dirichlet boundary condition. The figure shows that the lake level gradually increases during the selected simulation period. The water level observations have weak relation with the inflow from Ribb River which is shown in solid lines. To simulate the effect of lake water level on the flooding a constant water level (1784m) is specified as a downstream BC which allows for simulation of the free flow condition at the river outlet.

Initial Conditions

The model requires simulation of the initial condition that represents the actual hydraulic state of the river system at the onset of the actual simulation. In this work the initial conditions is entered by introducing a so called warm-up period. Subsequently initial states are evaluated by variations of water level at few calculation nodes which are located close to the upstream and downstream boundaries and in the middle reach of the river. After some trial simulations that served to test for the hydrodynamic flow behaviour of the model domain, it was decided that a warm-up period that covered some seven days was sufficient to achieve a somewhat stable hydraulic gradient in the system. The model was initialized using flow and water level observations for the time period August 1st to August 7th for 2006. The hydraulic states at August 7th served as initial condition and have been applied to simulate the August 8th peak flood event that has duration of four days and spans from the August 8th to August 11th. This event is referred hereafter as simulation period 1. The model simulated output for the 11th of August 2006 is specified as the initial condition for the 14th of August peak flood which was selected to compare simulation results against MODIS rapid response inundation map.

3.2.2. Surface Roughness

Surface roughness values as required by the model have been derived from the land use map of the floodplain and from the properties of river bed materials. The land use type which is dominant is cultivated area (Figure 1-3) and the river bed material is dominantly clay. The river bed consists of sedimented clay particles and causes much less friction to flow as compared to the floodplain. In this work and following (Arcement and Schneider, 1989) there are fixed roughness values assigned to the various land uses and river bed materials. To setup the model a Manning roughness

coefficient value of 0.03 for floodplain and 0.02 have been used. Figure 3-3 shows the distribution of surface roughness coefficients as used to set up the model. The common format for the surface roughness in SOBEK is the ASCI format.

Figure 3-3: Surface roughness layer used to setup the model.

3.2.3. Digital Elevation Model

The overland flow module of SOBEK uses the DEM of the floodplain and the river as a major input. In theory the model DEM should have a spatial resolution that allows for representation of larger scale properties that relate to the floodplain but ideally it also should represent small scale properties such as levees, dykes and obstructions by elevated roads. Clearly representing all properties at respective scales is not possible and much real world properties at spatial scales smaller than the selected DEM grid scale have to be ignored. As such a trade-off exists in selecting the grid scale and the detail and related elevation at which small scale as well as large properties can be represented. In this respects the quality of the DEM must be assessed to achieve a DEM with elevation error that may be considered acceptable for the flood problem at hand. In this regard, it is very important to consider the elevation of the DEM with respect to the actual elevation of the lake as the backflow from the lake to the floodplain highly depends on the elevation of the shore and areas around.

The DEM selected for this research is an ASTER DEM generated from ASTER scene (AST_L1A.003:2041822288) acquired on March 19, 2007 under no cloud cover. For the acquired date that is in the dry season, is river flow very low that on itself is a favourable condition to acquire the river topography. The DEM data products available are a 15m DEM and 30 m resolution DEM from the United State Geologic Survey (USGS). Both DEMs have a UTM coordinate system Zone 37 and datum WGS 84. Each DEM has a net size of about 60x60km, though the actual DEM file has an extension of 70x70km due to the slant of the satellite orbit. Figure 3-4 and 3-5 show the 15m and 30m DEM, respectively.

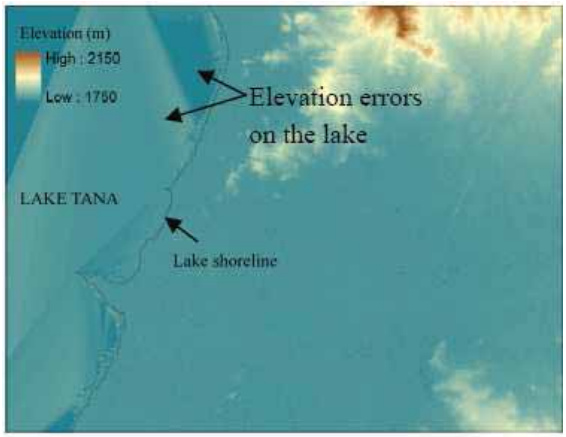

Figure 3-4: ASTER 15m resolution DEM

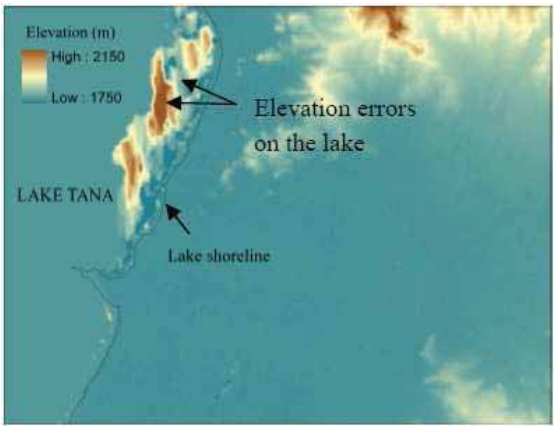

Figure 3-5: ASTER 30m resolution DEM

By erratic elevation distribution, the ASTER DEM which is available in 15m resolution has observation errors on the river course and on the lake surface. A similar problem is also observed on the 30m USGS produced DEM. Moreover, the USGS produced DEM is less capable of capturing the river topography than 15m DEM. Despite the problems, the 15m DEM is utilized to derive river cross sections to construct a representation of river topography. Figure 3-6 shows the elevation distribution along the river bed as sampled from ASTER 15m DEM. The elevations do not define the river gradient due to elevation errors along the river and lake shore.

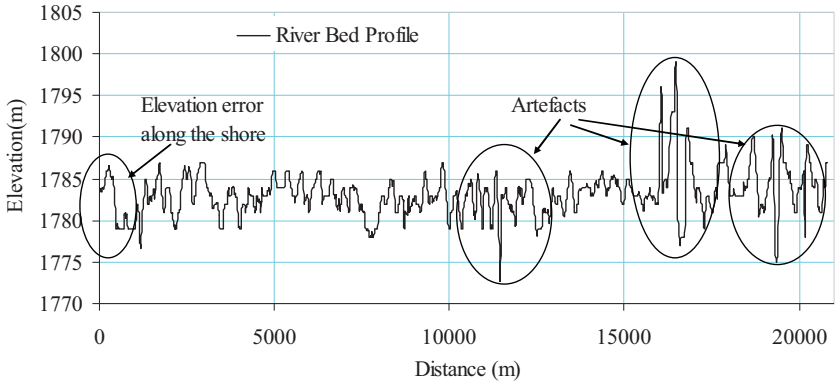

Figure 3-6: Elevations along the river centre line sampled from ASTER 15m DEM (The downstream end is the reference point, i.e. zero distance, for measuring the distance).

3.3. River Terrain Processing

3.3.1. Procedures to reconstruct river terrain

In this research ASTER based river cross sections along the river are compared against field measured cross-sections. This comparison indicated some mismatches between cross-sections and reliable cross-sections were selected or for further use while unreliable sections were rejected. Since the number of reliable observation was only limited it was found essential to reconstruct the entire river terrain to accurately represent the channel cross-sections. Reconstruction of the river channel and integrating its result in the raster DEM requires advanced GIS processing. By the comparison of ASTER DEM-field observed cross-sections only some twelve cross sections were selected that are shown in appendix A. These cross-sections

serve to fully reconstruct the channel bathymetry and related shape properties and the procedure involved a number of steps.

At first the selected locations of cross-sections by the ASTER DEM – field comparison are added and are indicated in Figure 3-7 by the solid lines. Secondly some five characteristic points (left bank, right bank, centre of channel and two points in between the centre and the banks) are added to these cross sections to allow reconstruction. Thirdly for specific locations along the river such as meanders where hydraulic flow properties largely change are new cross-sections added. For these cross-sections river bottom heights are defined for all five points that in the following are termed sample points. Channel height values for sample points that are in line to represent the centre of channel and two points in between the centre and the banks, receive average slope values by linear interpolation between upstream and downstream cross sections. .Since the average flood plain slope is some 0.03% also the channel has average slope of 0.03%. Channel height values for the sample points along the bank lines are simply defined from the DEM elevations. In this procedure all sample points now have assigned a height values and sample point represent a point map of river channel. This map now serves as input to an IDW interpolation procedure to construct a three dimensional river terrain model by means of a raster DEM. In Figure 3-7 the selected cross-sections are shown as well as geo-locations of all sample points that make up the cross-sections to be used for IWD interpolation.

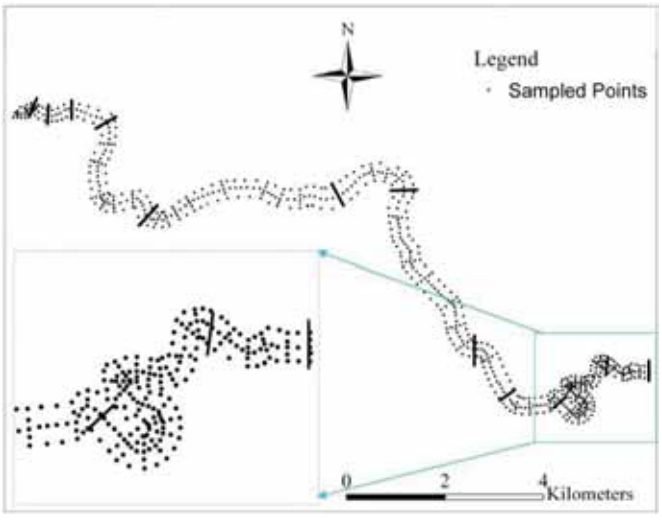

Figure 3-7 : The selected cross-sections and the point map which is used as an input to interpolation to create the river terrain.

3.3.2. Effects of Interpolation

The interpolation technique used to reconstruct the river terrain is the Inverse Distance weighting as suggested by Merwade et al. (2006). By such interpolation, the choice of search radius distance and weighting factor can have an effect on the result of the interpolation. In this study, tests for weight factors (w) within the range 0.5 to 6.0 have been analysed for a search radius 130 m. To assess which weight factor gives a good result, the interpolated layers are checked for the consistence of slope along different segment of the river reach while also the RMSE is calculated for selected points.

To calculate the slopes along each segment, the interpolated elevations along the centre line of the layer are sampled and grouped in ranges of distances. The centreline is divided in 4 segments of length of 5km while the slope is calculated for each segment. This is done for all segments and the slope distribution is expected to be consistent and should be close to 0.03% in the majority of the segments since this is the overall slope of the river terrain. The slopes obtained along each segment for different weighting are discussed in section 4-1.

For calculating the RMSE 20 points with known elevation are excluded from the centre line of the point map in Figure 3-7. This point map is then interpolated for the various weights that range between 0.5 and 6.0. Finally the interpolated elevations are compared against the known elevations at the corresponding locations and effects of deviations are calculated by means of the RMSE that is shown in equation 3-4. The most optimum interpolation result is indicated by the lowest value of the RMSE. Figure 3-8 shows the spatial distribution of excluded points with known elevations that are used to calculate the RMSE. The results of this procedure are discussed in section 4-1.

$$\mathbf{RMSE}=\sqrt{\frac{\sum_{i=1}^{N}(\hat{Y}_i - Y_i)^2}{N}} \qquad 3\text{-}4$$

where: $\hat{Y}_i$ Interpolated Elevation values (m)

Y_i Elevation values that are calculated using the slope (m)

N Number of sample points

Figure 3-8 : Distribution of validation points as extracted from the centre line of the river reach.

3.3.3. MODEL DEM preparation

For constructing the DEM for usage in the SOBEK flood model, the river terrain model has to be combined with the flood plain DEM. In the DEM the area covering the river channel and its banks is replaced by the newly constructed river terrain model. This is done in Integrated Land and Water Information System (ILWIS) through GIS techniques. The model DEM is constructed by integration of the river terrain with the floodplain DEM, which is referenced to the lake water level on the same date of image acquisition. The lake elevation on the DEM acquisition date is 1786.8 m amsl while the mean elevation of the shore of the lake obtained from the DEM is 1780.86 m. Since there is a difference between both elevations of some 5.94 m, such difference is added to the elevation of all pixels of the DEM to achieve a match between the two independent observations. The resulting DEM is then filtered twice using the 3x3 averaging low pass filters to smoothen the spikes and some depressions that were inherent in the ASTER DEM. Some 100m buffer zone in the 15m DEM is replaced by 30m DEM to reduce the effect of the elevation errors observed along the lake shore. The final DEM is shown and discussed in section 4-1.

3.4. Validation Data Sets

3.4.1. MODIS Rapid Response Flood Inundation Map

At Dartmouth Flood Observatory (DFO) flood inundation maps for the study area are available. Among the various tasks, this organisation advocates the widespread access of satellite-based measurements and maps, it facilitates research after causes of extreme flood events and it provides international warning of such floods. The Flood Observatory uses orbital remote sensing to detect and to map river discharges and river flooding patterns for areas across the globe. For this work the MODIS Rapid Response Inundation Map 3 of the August 2006 flooding in Lake Tana is obtained from the DFO archive and is referred to as the Master Index of Rapid Response Inundation Maps-2006 to 2008 glide number FL-2006_000123-SDN (http://www.dartmouth.edu/~floods/2006174Nile.html). The flood map is derived from MODIS image and was acquired under no cloud cover. The name of the product used is Lake Tana Rapid Response Flood inundation map 3. Figure 3-9 shows the inundation map of the flooding in August 14 (in dark) and August 19 (in gray) 2006 that is obtained from DFO. For the purpose of GIS analysis with simulated results the inundation map is georeferenced. The white colour boundaries show the flooding extent on August 14th which is digitized on the MODIS flood inundation map for the purpose of comparison (see section 4.3). The simulated flood extent of the August 14 flooding is compared against the inundation map using GIS operation.

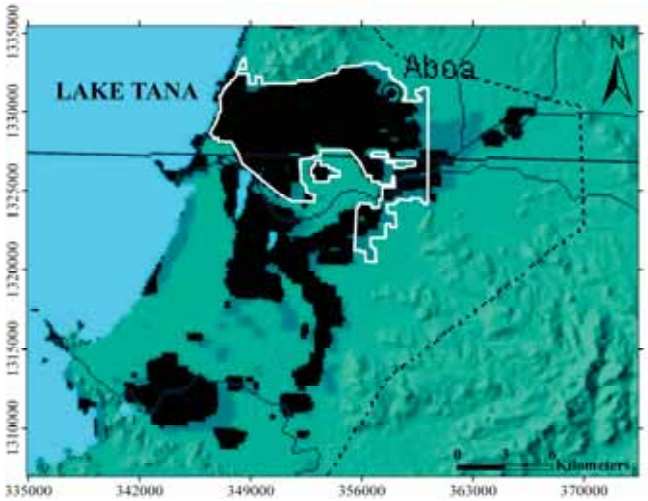

Figure 3-9 : MODIS flood inundation map of August 14 and 19, 2006 (DFO).

3.4.2. Historic Flood Depth Observations

The coordinates and the maximum flood depth data for the 2006 wet season are available. These data sets can be used to evaluate the prediction of the model results with regard to the simulated depths and the simulated inundation extent of the flooding. Figure 3-10 shows 12 spatially distributed flood depth observations for the August 2006 flood event with a maximum observed flood depth of 1.50 m. In this research these datasets are used to compare to water depth of the model results and are used to check if simulated flood areas also are observed at the location of observation points.

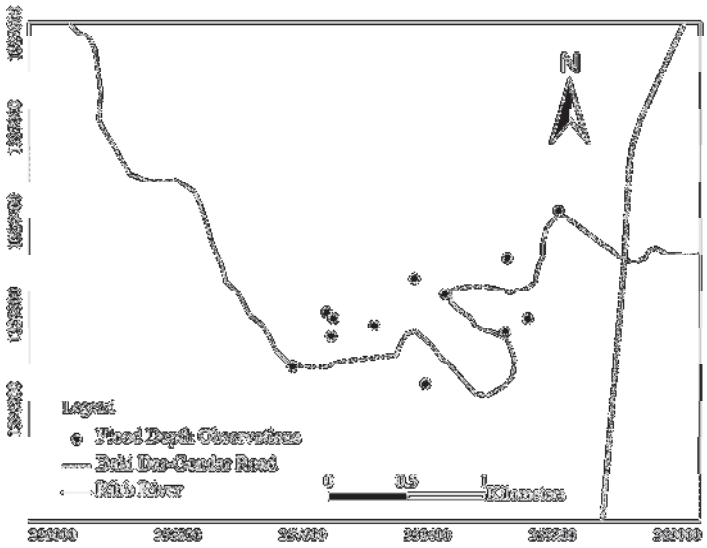

Figure 3-10: Distribution of historic flood depth observations along the Ribb River

4. Results and Discussions

4.1. Effect of interpolation in DEM accuracy

Accurate river cross-sections were only available at some locations along the river. As such, the terrain of the river between these cross-sections should be constructed by interpolating the elevation values. The effects of the selected weightings on the accuracy of the interpolation scheme are evaluated. Such allows selecting the best interpolation scheme that gives relatively accurate elevation values of the river terrain.

Table 4-1 shows the change in slope along the centreline of the river terrain that is interpolated. In the procedure is the total length of the river channel divided in 4 segments of 5 km length where and for each segment the slope is calculated as described in section 3.3.2. Table 4-1 shows results for inverse distance interpolation and indicates that for a weight factor of w = 4, the slope is consistent in three of the segments while the slope is largely inconsistent for w=1.The slope of the last segment for w = 4 is flatter than the results for other weightings used. Figure 4-2 shows the calculated RMSE of the interpolation results using different weights and indicates that that the RMSE decreases exponentially as w increases. For a search radius of 130 m, the figure also shows that the RMSE does not change largely for a weight factor larger than or equal to 4. The result suggests that a higher accuracy is achieved when a higher weight factor is selected as compared to a smaller weight factor. In this study, the weight factor 4 is selected for interpolation of cross sections.

Figure 4-2 shows that the RMSE decreases exponentially as w increases. For search radius of 130 m, the figure also shows that the RMSE does not change largely for weighting factor larger than or equal to 4. The result suggests that a better accuracy is achieved for larger weighting than smaller weighting. In this study, the weighting factor adopted for creating the river channel is 4.

Table 4-1: Effect of the IDW weights on the calculated slopes (%) for the four segment of the river

Segments	Weight(w)			
	1	2	3	4
1	0.04	0.03	0.03	0.03
2	0.03	0.03	0.03	0.03
3	0.03	0.03	0.03	0.03
4	-0.03	-0.01	-0.004	-0.002

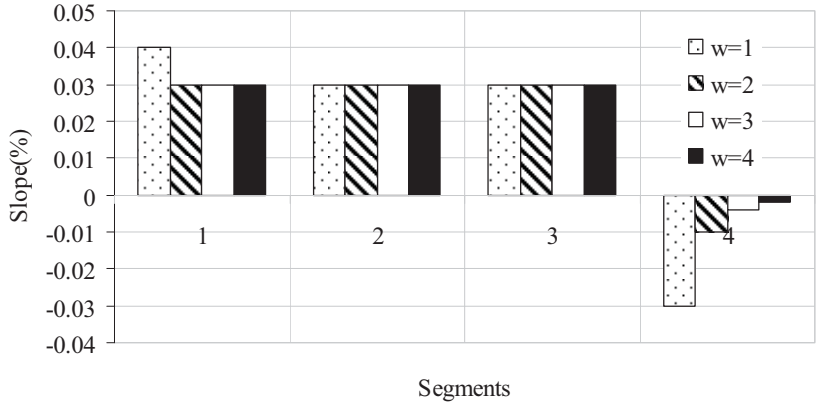

Figure 4-1: The distribution of slopes along different segments (upstream to downstream) along the centreline of the river calculated from the interpolated river channel.

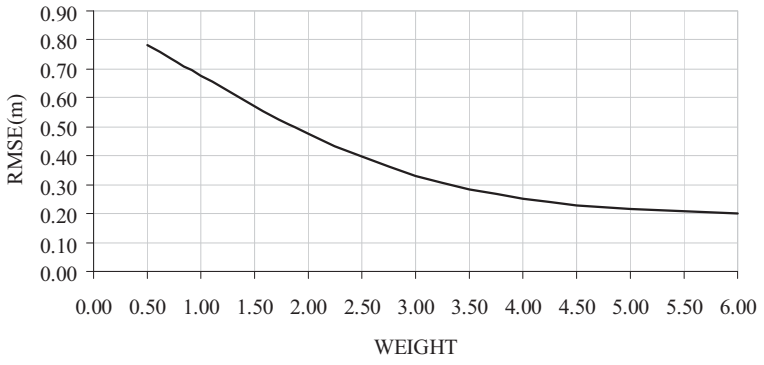

Figure 4-2: The root mean square error of interpolations for various weights

Figure 4-3 shows the river DEM which is created through IDW interpolation technique using a weighting factor of 4 and a search radius of 130m. Using a weighting factor larger than 4 gives a similar result.

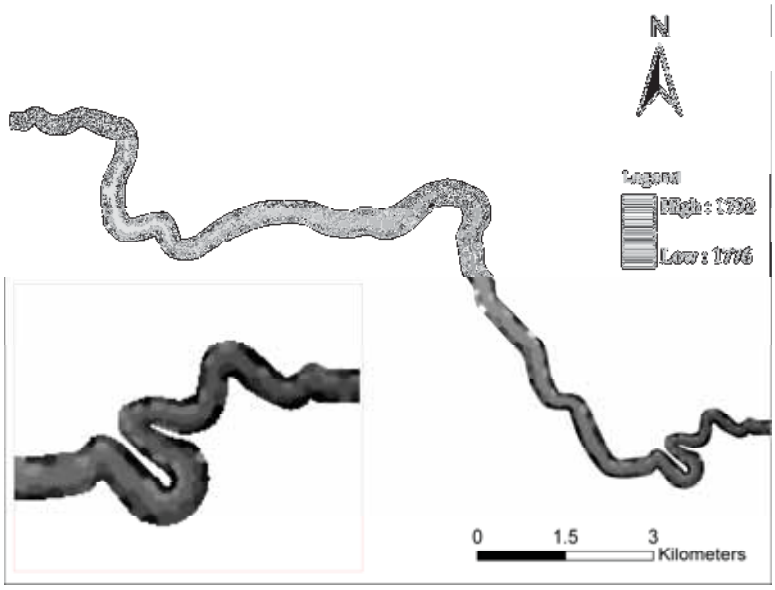

Figure 4-3: The river terrain model developed from interpolation of the calculated elevations.

Figure 4-4 shows the model DEM which is produced using the procedures in sections 3.3.2 and 3.3.3. The model DEM is exported to an ASCI file format to comply with the input requirements of SOBEK. Figure 4-5 shows the hill shade of the model DEM.

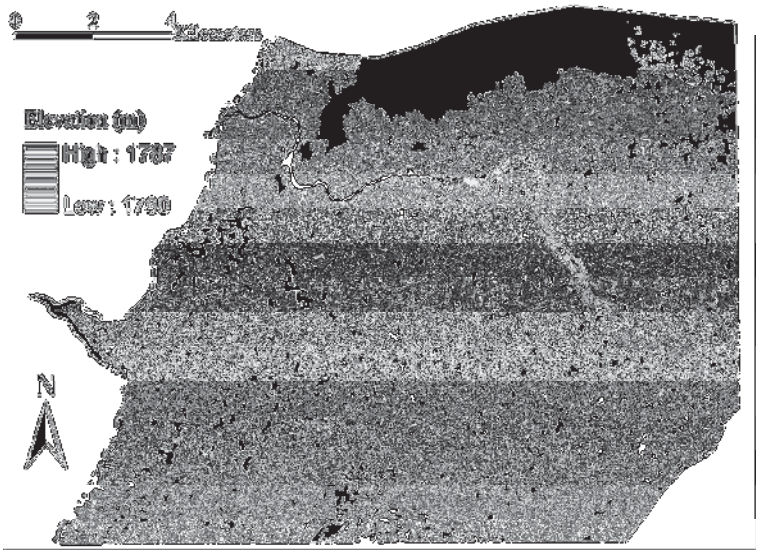

Figure 4-4: The DEM which is finally created by integrating the river channel and the floodplain.

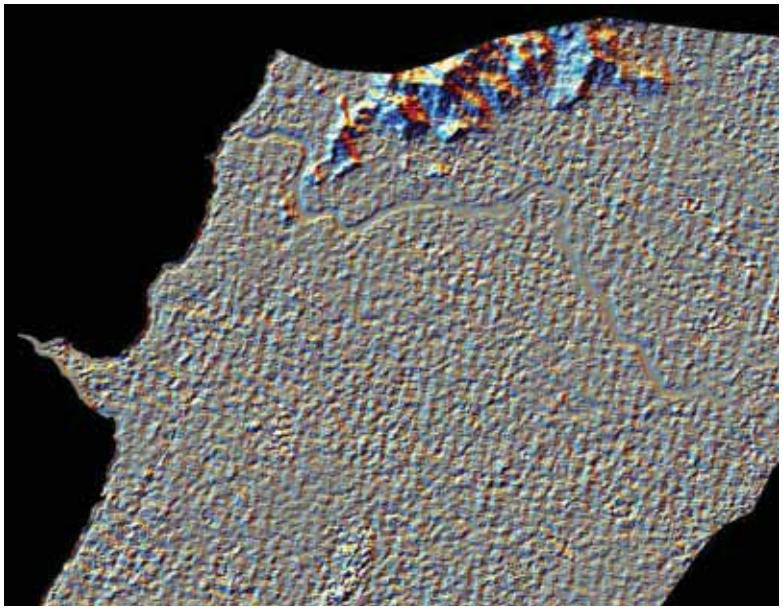

Figure 4-5: Hill shade view of river channel and the floodplain topography.

4.2. Simulated Flood Extent,Level, Depth and Velocity

Figure 4-6 shows the maximum flow depths and extent for simulation period 1 which starts on 07/08/2006 at 06:00:00 hr and ends on 11/08/2006 at 18:00:00 hr. The maximum size of the inundation area is 15.05 km^2 while some 83.5 % of the simulated flood extent has flood depths of less than 2.25 m. The simulated water levels range between 1791.13 m at the upstream and 1785.02 m amsl at the downstream end of the main river. The simulation result indicates large flooding extents in the upstream part of the river where the flow behaviour is mainly governed by the inflow from Ribb River. The flooding at the upstream reach of the river extends up to some 4.24 km outside the right bank(north) while it only stretches some 1.40 km outside the left bank (south) of the main river. Hereafter the term 'right bank' is referred to as the bank that is north of the river and 'left bank' stands for the bank south of the river. Some inundation is also observed in the middle reach of the river. The area which is inundated at the shore of the lake is minimal as compared to the flooding in the middle and the upstream reach of the river. In this work it is assumed that flooding in the downstream part is governed by the Lake water level and inflows from ungauged catchments that due to time constrains in had to be ignored. The flooding along the shore of the lake is observed only in the left bank side of the river and it propagates to a distance of some 1.13 km. In the middle reach flooding is observed up to some 1.33km from the river in the left bank side.

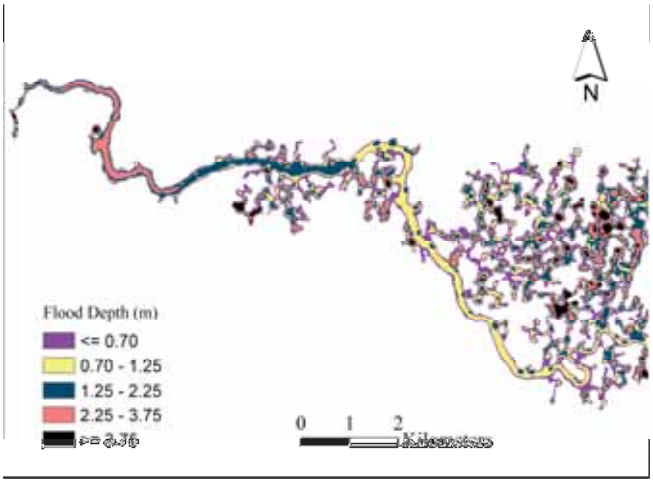

Figure 4-6: Maximum flood depth and extent for simulation period 1

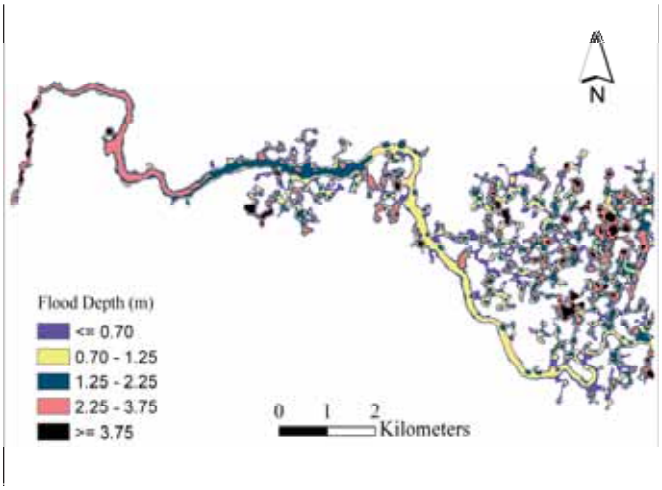

Figure 4-7: Maximum flood depths and extent for simulation period 2

Figure 4-7 shows the maximum flood depth and flood extent for simulation period 2 which starts on 11/08/2006 at 18:00:00 hr and ends on 16/08/2006 at 18:00:00 hr. Some 82 % of the simulated flood extent has flood depths of less than 2.25 m. In this simulation, the maximum water levels range between 1791.14 m at the upstream end and 1785.82 m amsl. at the downstream end of the main river. The area of the maximum inundation extent of simulation period 2 is 15.55 km^2. The flooding at the upstream river reach extends up to some 4.24 km in the right bank side of the river while it propagates some 1.40 km on the left bank. The flooding along the shore of the lake is also observed only at the left bank of the river and it propagates up to a distance of some 2.56km.

The pattern of the maximum inundation extent of simulation period 2 has not changed largely when compared to the pattern of the first simulation period. However, to have a better look at the difference between the two simulation periods, the deviation between both is calculated and is shown in Figure 4-8. Positive values in the figure indicate that the maximum depth increased during simulation period 2. Most deviations are within the 0.00 to 0.25 m. range. The peak flow of the first simulation period is higher than the second simulation while also the inundation depth and the extent are somewhat larger for the second simulation. Such difference shows that the flooding as simulated in the first simulation has not disappeared and the result reveals that the flooding characteristics of the second simulation period are

largely influenced by the flooding characteristics of the previous event. In terms of the spatial extent of flooding, there is an increase in flooding of some 0.50 km^2 which is an indication that the second peak flow has minimal effect on the flooding extent.

The two simulation results show that more flooding occurs in the right bank side of the river than the left side. The flooding extent which is in the right bank side of the river in the first 6.90 km of the upstream reach does not show any change for the two simulations. The effect of the lake level on the flooding extent is dominant along the shore in the left side of the river than the right side. The flooding along the shore of the lake is less compared to the upstream flooding. There is an overall increase of flooding extent of some 0.50 km^2 when comparing the two results and the changes in the flooding extent occur mainly close to the lake shore and some in the middle reach of the river (6-12 km from upstream boundary of the river). This indicates that the increase in the flooding extent in the second simulation is mainly due to the lake level.

The flooding characteristics of the two events are also summarized and then shown in Table 4-2. The model outputs for maximum flood level and velocity are shown in Appendix B

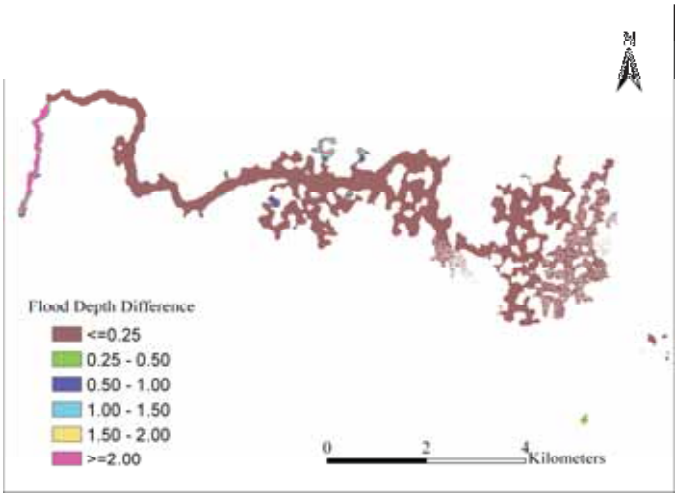

Figure 4-8 : The difference between the maximum depth of simulation period 1 and simulation period 2.

Table 4-2: Summary of maximum inundation extent, maximum flood depth and maximum flow velocity of simulation period 1 and simulation period 2

Flood period → Flood Characteristic ↓		Simulation period 1	Simulation period 2	Difference between periods
Flood extent (km^2)		15.05	15.55	0.50
Maximum flood Depth (m)	< 0.25	1.79	1.81	0.02
	0.25 – 0.5	1.69	1.73	0.03
	0.50 – 1.00	3.65	3.73	0.08
	1.00 – 2.00	4.66	4.74	0.08
	>=2.00	3.26	3.54	0.28
Maximum flood Velocity(m/sec)	< 0.25	12.05	12.77	0.72
	0.25 – 0.5	1.90	1.82	-0.09
	0.50 – 1.00	1.01	0.82	-0.19
	1.00 – 2.00	0.09	0.14	0.05
	>=2.00	0.00	0.00	0.00

4.3. Comparison of simulated inundation extent with MODIS flood map and historic flood observations

It is very important to evaluate the model for its capability in predicting the flooding. In this study, simulated inundation extent is compared against a MODIS flood inundation map product prepared by Dartmouth Flood Observatory. To do the comparison the model outputs are overlain by the MODIS inundation map by using GIS techniques and results are discussed below.

The Ribb river reach is divided into two flooding zones since most of the area in the middle and downstream reach of the river is mainly governed by flows from the surrounding ungauged catchments and the lake. The first zone is the area in the upstream reach of the river in which flooding is mainly governed by Ribb River and the second zone is the areas in the middle and lower reach of the river where flow is governed by the river, the lake and flow from the surrounding catchments. As most of the area in the middle and downstream reach of the river are mainly governed by runoff from surrounding areas and the lake back-water effects, the second zone is not considered for the purpose of comparison with MODIS inundation map.

The area that is selected for comparison extends to a distance of some 6.90 km along the river from upstream boundary as shown figure 4-9 and 4-10. The simulated flooding extent in the comparison zone is some 9.62 km^2 while the extent in MODIS inundation map is 29.60 km^2. In figure 4-9 the dark area shows the simulated inundation area that matches with the MODIS inundation map and has an extent of 9.02 km^2. The dark areas in figure 4-10 show the simulated flooding extent that was shown as dry area in the MODIS inundation map. The size of this area is 0.60 km^2 and it indicates overestimation by the model. The comparison result indicates that 30.50 % of MODIS flooding extent is explained by the flood extent that is simulated for the flow of Ribb River for simulation period 2.

In this study, the effect or the contribution of Ribb flow on the flooding extent is discussed. As it can be seen from the MODIS inundation map, the area which is inundated is much larger than the model simulation. This can be seen from three different perspectives. Firstly, the MODIS inundation map may overestimate the flooding extent by reporting some wetted surface as a flooded area. Secondly, the effect of rainfall on the floodplain is not modelled. In SMEC (2007) it is indicated that the floodplain area is characterized by low infiltration rates (less than 5mm/day) and such characteristic can cause significant flooding due to direct runoff. The flooding that was caused by the rainfall on the floodplain is included in the MODIS inundation map. Thirdly, the contribution of ungauged flows to the flooding is not modelled due to time constrains in this thesis work. However, the contribution of ungauged flows clearly is included in MODIS inundation map. The area of the ungauged catchments that contributes to the flooding in the comparison area, which is the upstream part of the floodplain, is 15 % of the area of Ribb catchment. The square dots in figure 4-9 show the location of the outlets of ungauged catchments. Even if the model simulation is able to predict the flooding (sufficiently) accurately, there could be a certain level of mismatch during comparison with MODIS or any other flood observation data but the difference should be acceptable. Also errors in the data to be used for the comparison should be considered. For instance, there are some areas in MODIS inundation map which are mapped as ‘no-flooding’ though these areas include the river course itself and this indicates that there is also uncertainty in MODIS inundation map.

It can be inferred from the model output that the model is able to predict the flooding pattern and extent to some acceptable level. The model correctly reproduced the flooding in the areas where flooding frequently displaces people which is in the northern part of the upstream 6km reach of Ribb river.

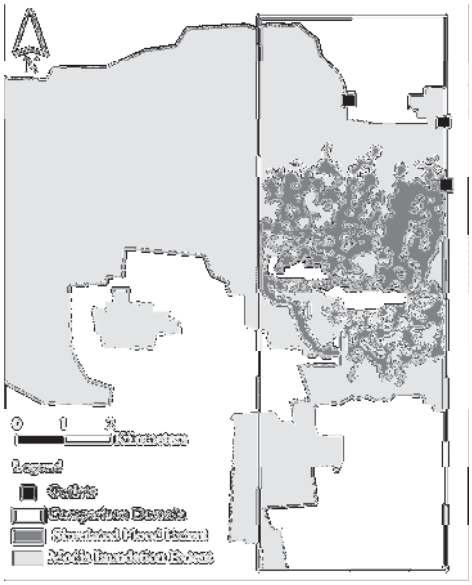

Figure 4-9: Dark areas show the correctly predicted areas by the model when compared against MODIS inundation map of 14th of August, 2006.

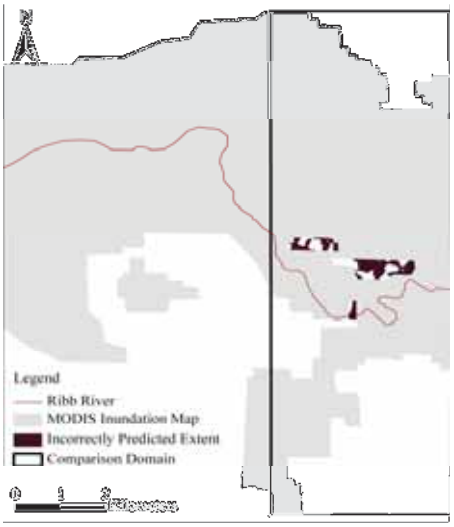

Figure 4-10: The flood extent that is incorrectly predicted when compared against MODIS flood map of 14th of August, 2006.

The comparison of historic flood observations with the simulated flooding extent reveals that 8 out of 12 observations described in section 3.4.2 lie in the simulated flooding extent. The remaining 4 observation points are out side the simulated flood extent and as such indicate mismatch with the simulation result. The reason for the mismatch is that the collected flood observations are for the maximum flood depth and extent in August 2006 flooding and does not necessarily indicate the flood depth and extent in simulation period 1 and simulation period 2. As it is shown in figure 3-2 of the previous chapter there are some peak flows that were observed outside the range of the simulated periods, for instance the August 22 peak flow is the maximum of all peak flows in the wet season. However, this event was not simulated in this study. Figure 4-11 shows the observed maximum flood depth for the 2006 wet season and the simulated maximum depth for August 14th 2006 flood event. The figure indicates that most of the predicted depths do not match with the observations.

Figure 4-11 shows that the simulated flood depth at observation point 3 is higher than the maximum observed depth of the wet season. This indicates that either the observation is not reliable as it is not an automated flood mark observation or the model result is not reliable at this location as such a case where there are some elevation errors in the DEM. At observation points 1, 5, 7, 11 and 12 the model estimates are better (0 to 0.25 m less than the observed depth). Observation points without simulated depths are the places where the model predictions are less accurate when compared to the MODIS inundation map. The flooding due to Ribb River at these locations for the simulated flood events may not inundate these locations and the observed flooding in MODIS inundation map at the corresponding location can be caused by either ungauged flows or rainfall on the floodplain or floodings that are outside the periods described in section 4.2.

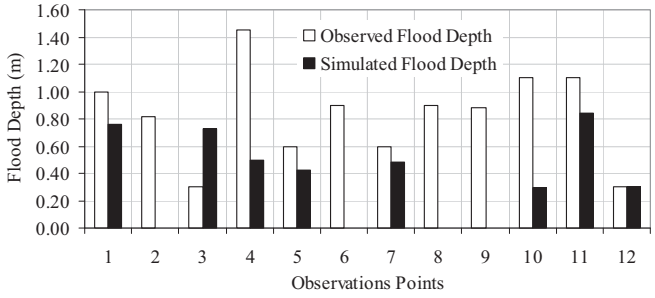

Figure 4-11: Comparison between the maximum of flood depths observed in the 2006 wet season and the simulated flood depth for 14th of August flood event

The comparisons of the model results with flood depth observations indicates that the model generally underestimates the flood depths as observed by the local people based on their observations on the maximum flood depth that occurred in the wet season of 2006. For better comparison of the observed maximum flood depths with modelled depths, the simulation period should cover the whole period in August and September which are likely to produce the maximum inundation. The simulations' periods in the study are limited to 17 days because of high demand of computational time.

4.4. Effect of Interpolation on Flood Inundation Extent

The effect of IDW interpolation of the river terrain model (Section 4-1) on the flooding characteristics is evaluated for simulation period 2 using two river terrain DEMs that are constructed using weight factors of w = 1.0 and w = 4.0. Figure 4-12 shows maximum flood extent and flood depth for simulation period 2 that is simulated using the river terrain DEM that is interpolated using a weight of 1.0. The result shows that the flood area increases when this DEM is used as an input to SOBEK. Small weight of IDW increased the effect of bank elevations on the interpolated river terrain. Since the banks have higher elevation than the centreline, the effect of lower weight is that it causes small conveyance that result in large overflow causing inundation in the floodplain. A DEM input that is created with a weight factor of 1.0 caused an additional 2.49 km^2 inundation area as compared to applying a weight factor of 4.0. The percentage of the increase in simulated inundation extent by the selected distance weight factor is some 27.56%.

Figure 4-13 shows the difference in the flooding extents (see the other cases as well) due to the effect of interpolation on the accuracy of the river terrain model. The black areas show the difference between the simulated flooding extents for DEM inputs that are created using weightings of 1.0 and 4.0. The flooding extent for w = 4.0 is shown in figure 4-7. Table 4-4 shows the summary of the maximum flood depth, velocity and extent for weighting of 1.00 and 4.0. The model outputs for maximum flood level and velocity for a DEM of w =1.0 are shown in Appendix C.

The effect of interpolation on the flooding extent shows that the results of hydrodynamic modelling are affected by geometric representations of channel bathymetry as Merwade et al. (2008) explained.

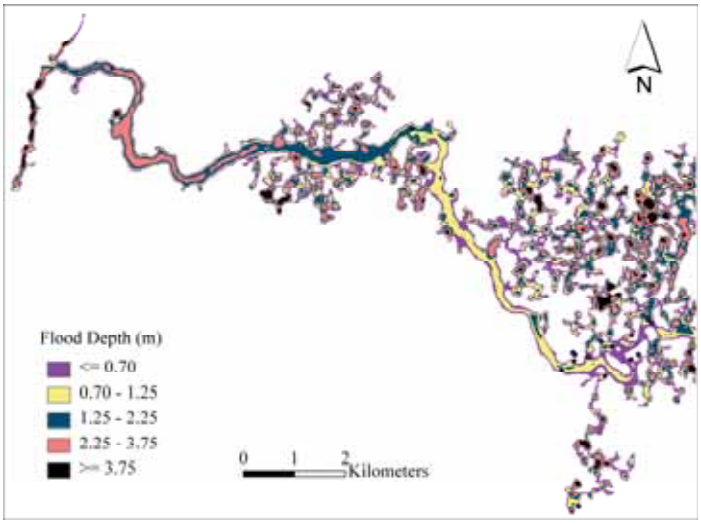

Figure 4-12 : Maximum flood depth and extent observed for w =1.0

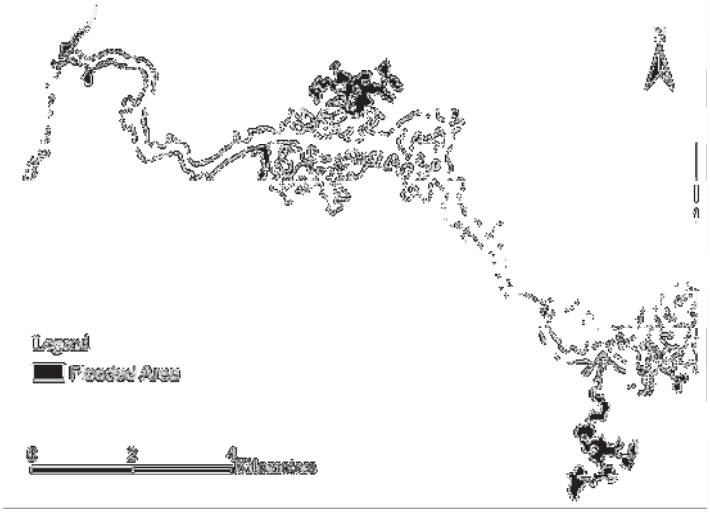

Figure 4-13 : The difference in maximum flood inundation extent due to interpolation effect.

Table 4-3: Summary of the effects of interpolation (for w=1.0 and w=4.0) on the maximum inundation extent, depth and flow velocity that are simulated with SOBEK.

	Weight Factor	1.00	4.00	
Flooding characteristics		Flood extent (km^2)	Flood extent (km^2)	Difference in flood extent(km^2)
Inundation extent		18.04	15.55	2.49
Maximum Flood Depth (m)	< 0.25	2.21	1.81	0.40
	0.25 – 0.50	2.08	1.73	0.35
	0.50 – 1.00	4.09	3.73	0.36
	1.00 – 2.00	5.49	4.74	0.75
	>=2.00	4.16	3.54	0.62
Maximum Flood Velocity(m/s)	< 0.25	15.48	12.77	2.71
	0.25 – 0.5	1.75	1.82	-0.07
	0.50 – 1.00	0.73	0.82	-0.09
	1.00 – 2.00	0.07	0.14	-0.07
	>=2.00	0.00	0.00	0.00

4.5. Effect of Lake Water Level on Flood Inundation Extent

The study of flooding allows to differentiate between the stretch of the floodplain that is inundated by the upstream flows from Ribb river and the stretch of the floodplain that is mainly inundate by the effect of relatively high lake water levels. In this study, the flooding of simulation period 2 is analysed by deliberately specifying the downstream boundary condition as a constant head (1784.0 m) as such head allows for the simulation of a hydraulically free flow condition at the river outlet so as to ignore the effect of lake level. The simulated flood extent is compared to a simulation result that used the actual water level as a downstream BC as shown in Figure 4-7 of section 4.2.

Figure 4-14 shows the flooding pattern when the effect of the lake is ignored, i.e. for a hydraulically free flow condition. The figure shows that inflow of Ribb River that is the upstream boundary condition, mainly affects flooding in the upstream reach with some minor effect in the middle reach. Figure 4-15 shows the contribution of the lake level on the overall flooding extent. The black areas show the difference in the inundated area between the hydraulic free flow simulation and the simulation

when observed lake water level is specified as downstream boundary condition. The black areas in the figure are inundations caused by the observed lake water level and reveal that the lake effect on the flooding can propagate to the middle reach of the river that is 6 to 9km upstream from the lake. The percentage contribution of Lake Tana on the simulated flooding is some 8.55 %.

The flooding characteristics due to the effect of the lake are also summarized and then shown in Table 4-5. The simulated flood level and velocity for hydraulic free flow condition are shown in Appendix D.

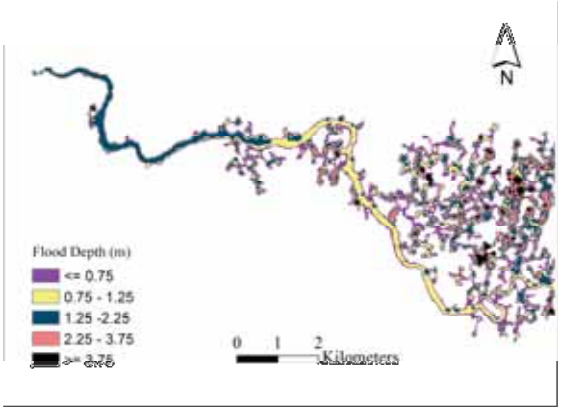

Figure 4-14 : Maximum flood level and extent observed for hydraulic free flow condition

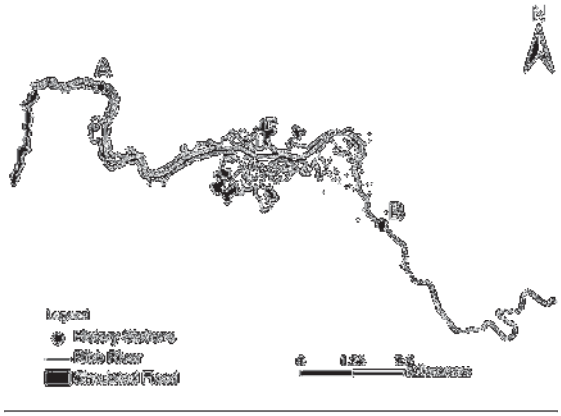

Figure 4-15: Maximum flood extent due to the effect of lake level. The black areas indicate the inundation area by the lake water effect.

Table 4-4 : Summary of the effect of lake on maximum inundation extent, maximum depth and maximum flow velocity.

Flooding characteristics		For actual Lake water level Simulation	For Hydraulic Free Flow Condition	Difference in flood extent (km^2)
Inundation extent(km^2)		15.55	14.22	1.33
Maximum Flood Depth(m)	< 0.25	1.81	1.72	0.09
	0.25 – 0.50	1.73	1.68	0.05
	0.50 – 1.00	3.73	3.62	0.11
	1.00 – 2.00	4.74	4.64	0.10
	>=2.00	3.54	2.58	0.96
Maximum Flood Velocity (m/s)	< 0.25	12.77	11.23	1.54
	0.25 – 0.5	1.82	1.65	0.17
	0.50 – 1.00	0.82	1.24	-0.42
	1.00 – 2.00	0.14	0.11	0.03
	>=2.00	0.00	0.00	0.00

The dark cross symbols at nodes A and B in figure 4-15 are the locations of at which historic flood levels are available. History node A is located at the downstream reach 2km away the river outlet when measured along the river and history node B is located 7 km from the upstream boundary of the river when measured along the river. These stations are selected to study how far the effect of the lake can propagate along the river.

In figure 4-16, the solid line shows the simulated flood depths when the observed lake level is specified as downstream boundary condition while the broken lines show simulation result when hydraulically free flow is specified at the downstream boundary. These lines indicate the small difference in flood depths due to the downstream boundary condition which ranges from 0.006 to 0.011 m at history node B. This proves that the lake does not have any significant effect on the flood depths for a location upstream from this point onwards that is in the first 6 km from the upstream boundary of the river. In other words, the effect of the lake dissipates after propagating 13 km along the river.

In figure 4-17, the solid line shows the simulated flood depths at history node A when the observed lake level is specified as the downstream boundary condition while the broken lines show the simulation result when hydraulically free flow is

specified at the downstream boundary. The deviation in the simulated flood depths between the two lines ranges from 0.55 to 0.74 m which indicates the effect of the lake on the flood depths that is dominant near the lake shore. The simulated flood depths are higher when the lake effect is considered and indicates the effect of the selected downstream boundary condition

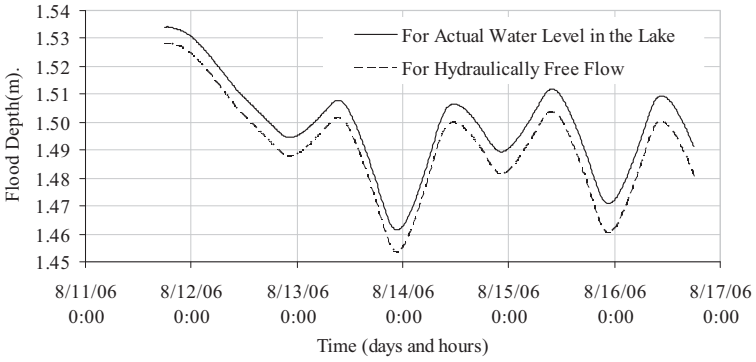

Figure 4-16: The simulated flood depths at 13 km from the downstream boundary for the selected boundary condition types

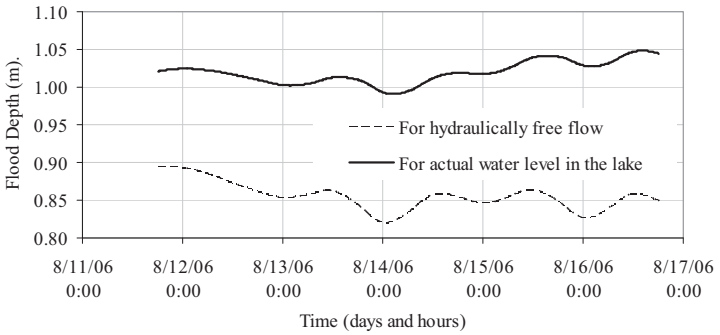

Figure 4-17: The simulated flood depths at 2 km from the downstream boundary for the selected boundary condition types.

5. Conclusions and Recommendations

In this study, a 2D hydrodynamic flood model (SOBEK) is applied to study the August 2006 flooding in Ribb Catchment while an ASTER DEM of 15 m resolution serves as a model input to represent the topography. The same DEM is used to construct River Terrain models to represent channel topography. Effects of IDW interpolation in the procedure to construct the river terrain model are also studied through cross-validation. Validation data sets to evaluate model results were obtained from remote sensing and ground-based observations. These data sets are MODIS rapid response inundation maps and historic flood observations.

GIS operations are applied to re-construct the river terrain since most of the river cross sections that were derived from the ASTER DEM did not match with field observations of the river cross-sections. About twelve cross sections are obtained at somewhat equal intervals of the 20 km reach and served as input to a procedure to estimated elevations of intermediate channel points that are sampled along the river. The inverse distance weighting algorithm of interpolation is used in the procedure and different weights are tested so as to minimise the effect of interpolation. Interpolation with a weight factor of 4 is found to create the terrain with lowest RMSE of 0.20 while smaller weights were found to increase the error.

The simulated flood characteristics reveal that large flooding is observed in the upstream end of the river where many people were displaced during the August 2006 flooding. For these areas, the simulated flood extent was found being overlapped by a MODIS inundation map of the same events. This study indicates that some 30.50 % of MODIS inundation extent can be explained by the simulated flooding extent for August 14th flooding event of the Ribb River. The remaining inundation extent in the MODIS inundation map can be caused by ungauged flows, rainfall on the floodplains and uncertainties related to construction of the MODIS inundation map. The comparison of historic flood observations against the simulated flooding extent reveals that 8 out of 12 observations that reported flooding lie in the simulated flooding extent of the August 14th event. The simulation results show that large floodings occur at the right bank, i.e. north, of the river as compared to the left bank.

It is observed that the simulated flood extent and other flood characteristics change when DEMs are created with different weight factor for interpolation. Interpolation of the river terrain using w = 1.0 resulted in an increase in flood extent. The

percentage of the increase in flooding extent by the interpolation effect is some 27.56%. The interpolation result for w=1 in section 4.1 show that the effect of bank elevations is observed at some locations along the centre line of the river terrain. This causes small conveyance in the channel and affects the river gradient to some extent causing over flow of the river.

The simulation results show that the effect of Lake Tana water level propagates up to 13 km upstream of the lake when measured along the river. The contribution of Lake Tana back-water effects on the simulated flooding extent is some 8.55 %. The flooding due to the lake is along the shore and middle reach of the river that is up to 6 to 9 km upstream from the lake. The lake causes flooding along its shore and along Ribb River by affecting the flooding characteristics of the river. The flooding extent due to the effect of the lake level is 1.33 km^2 which is 8.55% of the simulated flooding or 9.35% simulated flooding due to Ribb River. The contribution of Ribb flow in the simulated flood extent is some 14.22 km^2. The distribution of the flood by such inflow shows that some 67.64% of the inundation occurs in the area within a distance of 6 km from the upstream boundary where flooding is mainly in the right bank of the river.

In this study, one of the major limitations was the long computation time by the SOBEK model. For a simulation period of 16 days, for instance, computation time was some 7 days on a 2.13GHz Pentium IV PC. Obviously, producing a sufficient number of simulations to match all research objectives is highly dependent on available time. In the study, the computational time has become a barrier for accurate calibration of the model. However, the accuracy of the simulation result may be considered acceptable when compared against MODIS flood extent map.

The effect of different search radius and other interpolation techniques are left for future studies. Towards future research after flooding in Ribb River, it is advised to simulate also the effect of direct runoff from ungauged catchments. It is also recommended to model the flooding using high resolution DEMs such as LiDAR for better representation of topography

In developing countries such as Ethiopia where the availability of river cross-section data at high resolutions is limited, the use of satellite derived topographic data such as ASTER DEMs as source river cross-section data is inevitable. High resolution data such as LiDAR are not common in such a country and public domain topographic data have to be used. As such it is very important to extract cross-sections and channel alignments with data collected by a field survey.

The results of this study suggest that ASTER DEM can be used to estimate flooding characteristics in Ribb Catchment using the SOBEK hydrodynamic flood model. The use of advanced GIS operations, however, is inevitable. It also suggests that SOBEK is a powerful tool in predicting flooding characteristics of the Ribb floodplain. In addition, this study proves that geometric descriptions of channel topography have significant effect on the outputs of hydrodynamic models. This study reveals that any change in the water level of Lake Tana affects the flooding pattern in the floodplain.

APPENDIX

Appendix A: Cross sections selected from ASTER 15 m DEM (where CS1 is the cross-section at downstream end and CS12 is the cross-section at upstream end)

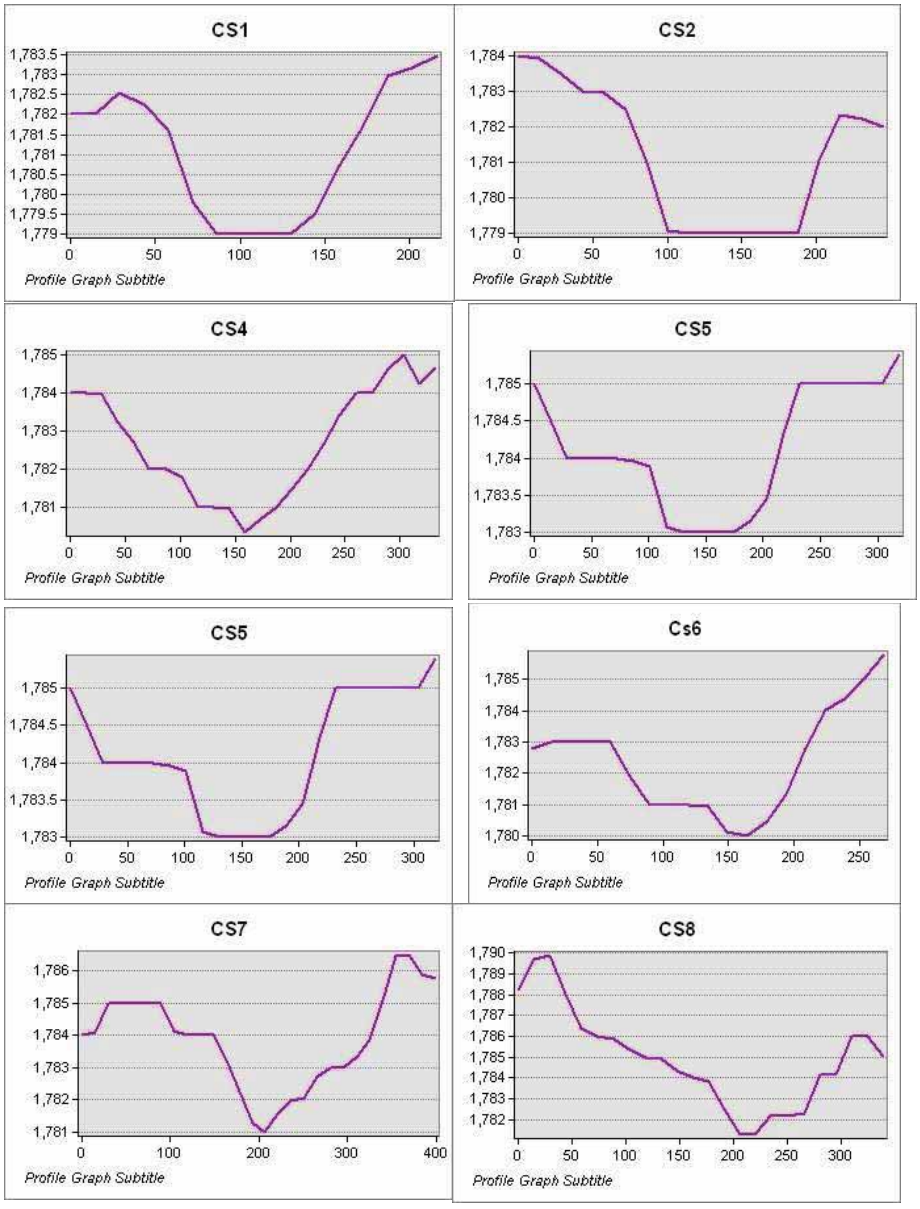

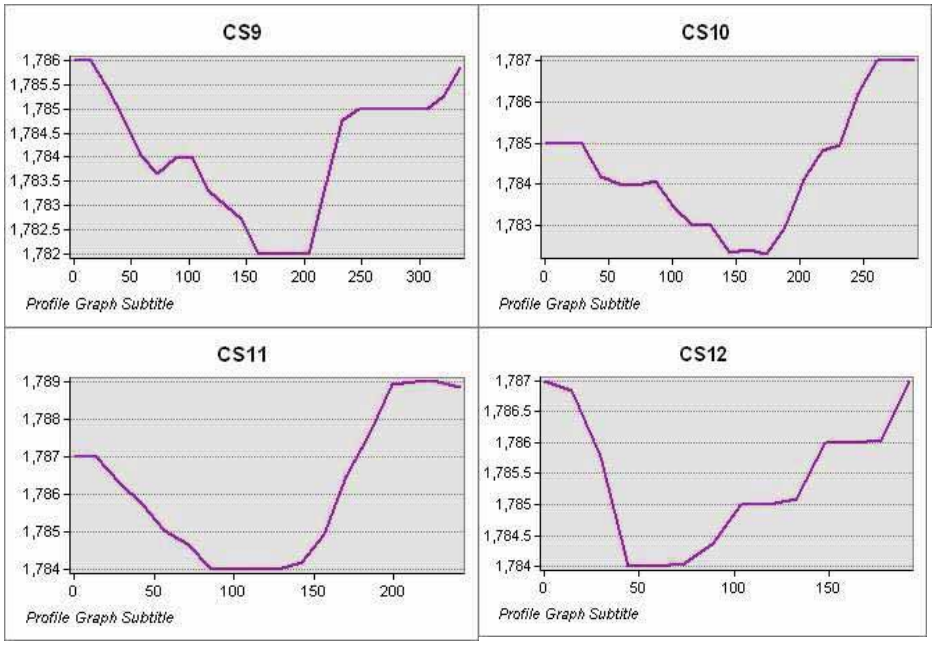
CS9
1,786
1,785.5
1,785
1,784.5
1,784
1,783.5
1,783
1,782.5
1,782
0
50
100
150
200
250
300
Profile Graph Subtitle
CS10
1,787
1,786
1,785
1,784
1,783
0
50
100
150
200
250
Profile Graph Subtitle
CS11
1,789
1,788
1,787
1,786
1,785
1,784
0
50
100
150
200
Profile Graph Subtitle
CS12
1,787
1,786.5
1,786
1,785.5
1,785
1,784.5
1,784
0
50
100
150
Profile Graph Subtitle

Appendix B: The model outputs for flood level and velocity.

a. Maximum flood velocity for simulation period 1 (m/s)

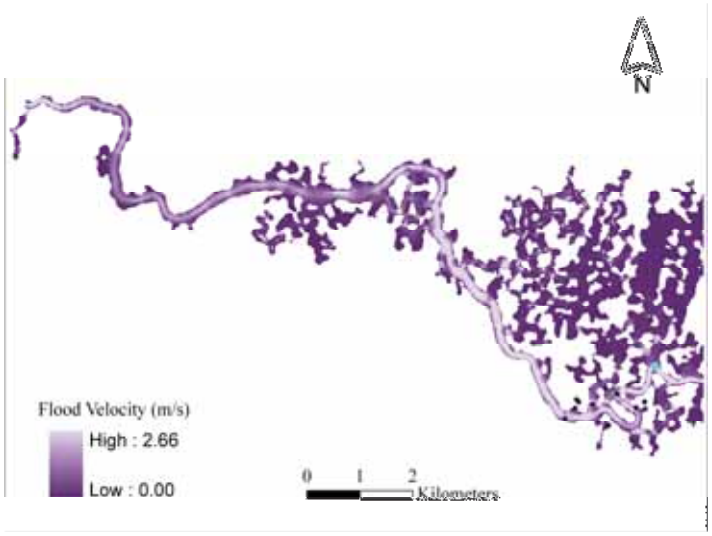

b. Maximum flood velocity for simulation period 2 (m/s)

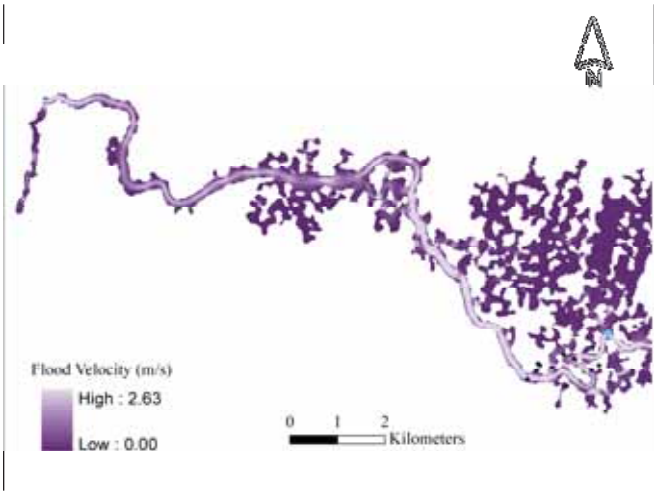

c. Maximum flood level for simulation period 1(m)

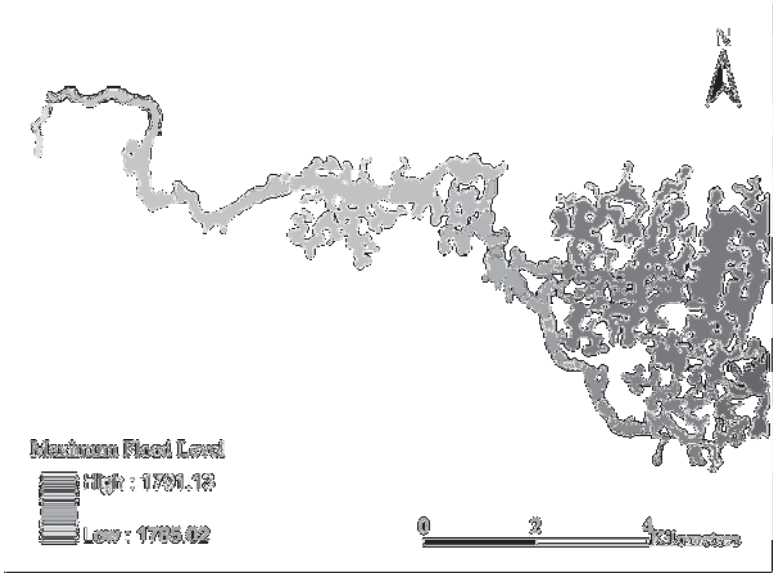

d. Maximum flood level for simulation period 2(m)

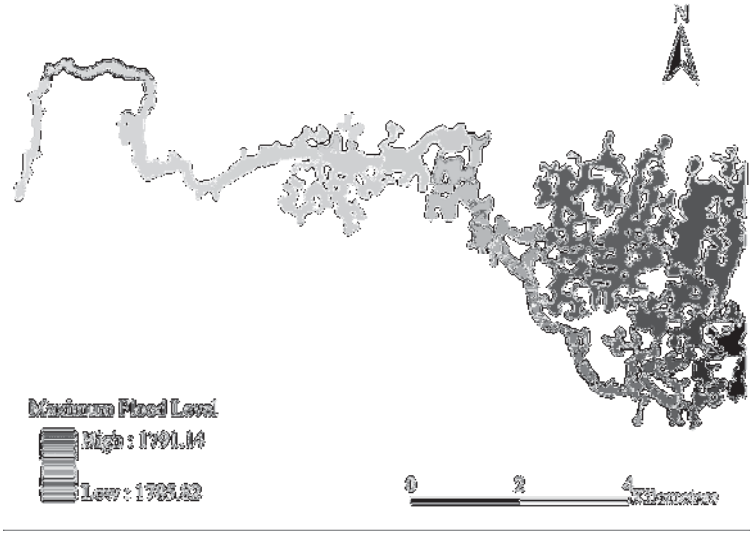

Appendix C: Effects of interpolation on flood velocity and flood level

a. Maximum flood velocity (m/s) for w=1.0

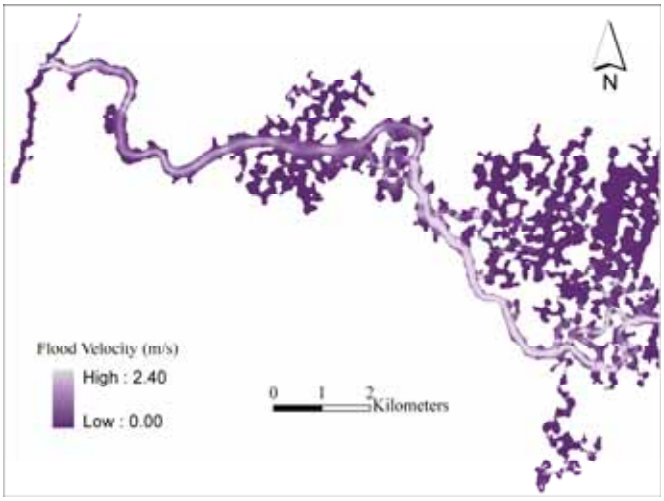

b. Maximum flood velocity (m/s) for w= 4.0

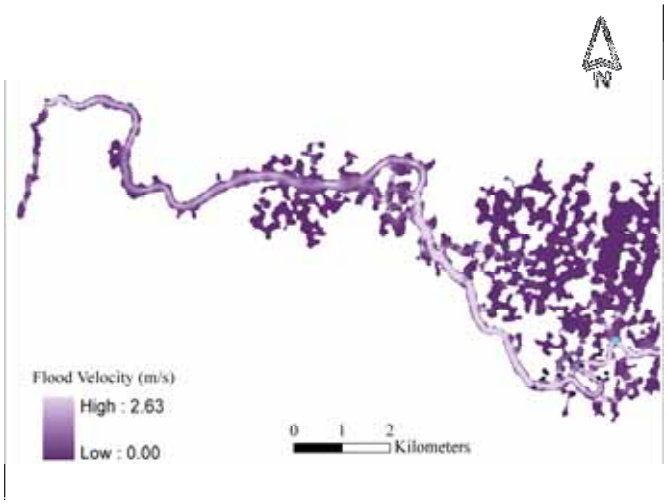

c. Maximum flood level (m) for w=1.0

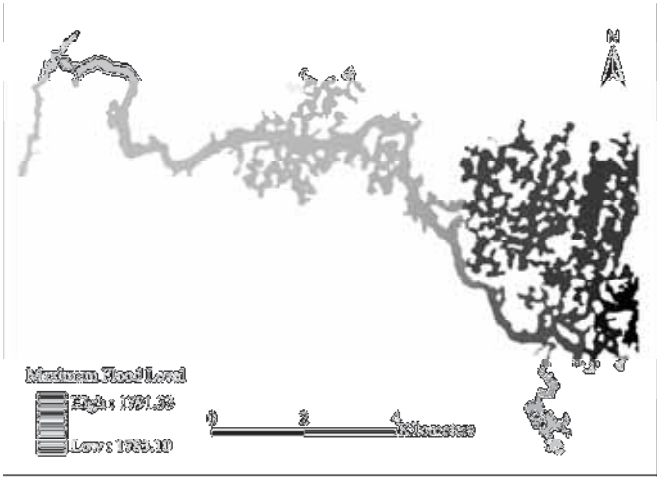

d. Maximum flood level (m) for w= 4.0

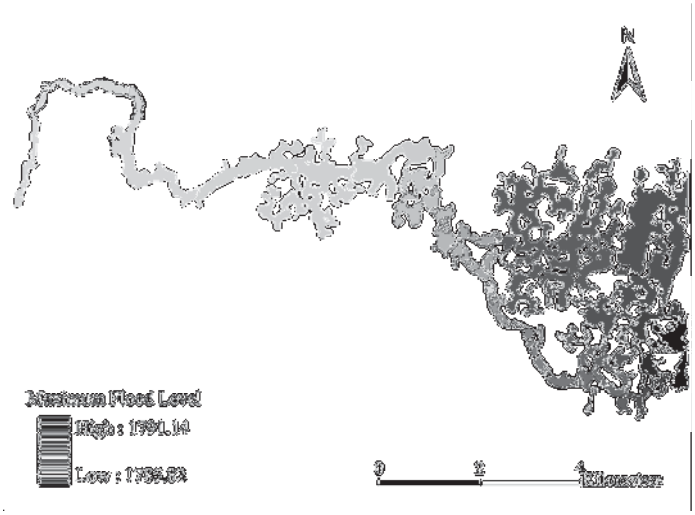

Appendix D: Effect of the lake on flood depth and velocity.

a. Maximum flood velocity (m/s) for hydraulically free flow

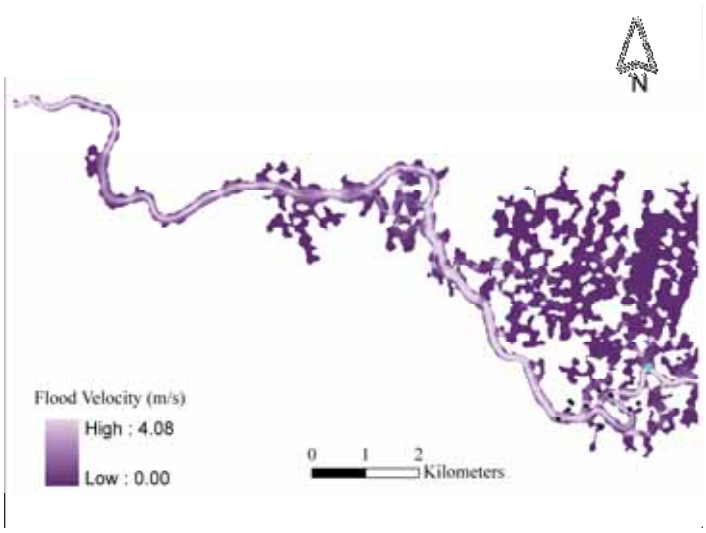

b. Maximum flood velocity (m/s) for actual lake water level simulation

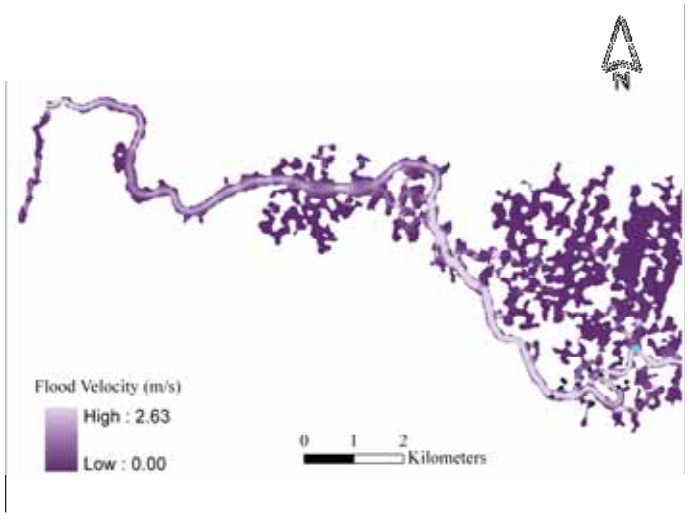

c. Maximum flood level (m) for hydraulically free flow

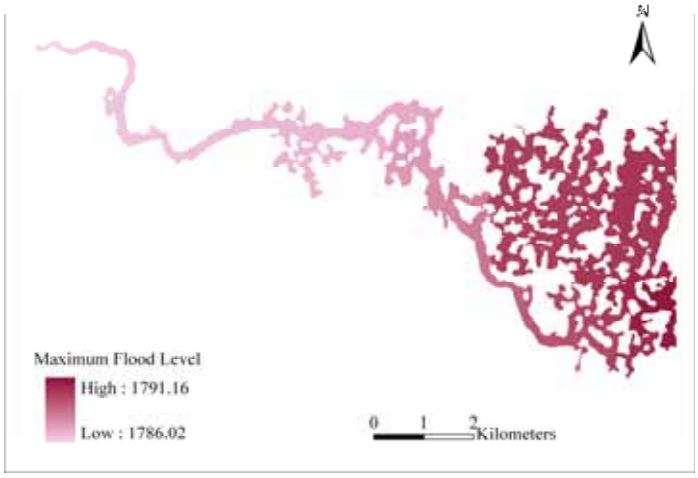

d. Maximum flood level (m) for actual lake water level simulation

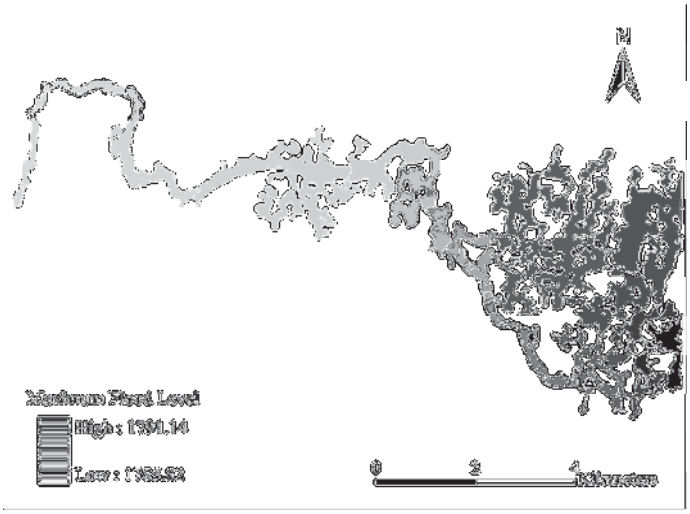

References

Arcement, G.J. and Schneider, V.R., 1989, "Guide For Selecting Manning's Roughness Coefficients For Natural Channels And Floodplains". US Geological Survey, Water Supply Paper 2339.

Assefa, K.A., Andel, S.V. and Jonoski, A., 2008, Flood Forecasting and Early Warning in Lake Tana Sub Basin,Upper Blue Nile, Ethiopia. WaterMill Working Paper Series,no.16.

.Bates, P.D., 2004, Remote sensing and flood inundation modelling. Hydrological Processes, 18: 2593-2597.

Beven, K., 1989, Changing ideas in hydrology: the case of physically based distributed models. Journal of Hydrology, 105: 79–102.

Chow, V.T., 1959, Open channel hydraulics, McGraw-Hill, New York.

Cuartero, A., Felicísimo, A.M. and Ariza, F.J., 2004, Accuracy of DEM Generation from TERRA-ASTER Stereo Data. International Archives of Photogrammetry and Remote Sensing, 35: 559–563.

Cunderlik, J.M. and Simonovic, S.P., 2003, Assessment of water resources risk and vulnerability to changing climatic conditions: Hydrologic model selection for the cfcas project. Report No. I, The University of Western Ontario, London, Ontario, Canada.

Dhondia, J.F. and Stelling, G.S., 2002, Application of one dimensional- two dimensional integrated hydraulic model for flood simulation and damage assessment. Proceedings of the Fifth International Conference on Hydroinformatics, Cardiff, 1: 265–276.

Dyhouse, G., Benn, J.R. and Jennifer Hatchett, P.E., 2003, Floodplain Modeling Using HEC-RAS. US Army Corps of Engineers.

Fujisada, H., Iwasaki, A. and Hara, S., 2001, ASTER stereo system performance. International Society for Optical Engineering: 39-49.

Haile, A.T. and Rientjes, T.H.M., 2005, Effects of LIDAR DEM Resolution in Flood Modelling : A Model Sensetivity Study for the city of Tegucigalpa,Honduras. MG Vosselman and C. Brenner (Editors), 3: 168-173.

Hirano, A., Welch, R. and Lang, H., 2003, Mapping from ASTER stereo image data: DEM validation and accuracy assessment. ISPRS Journal of Photogrammetry and Remote Sensing, 57: 356-370.

Horritt, M.S. and Bates, P.D., 2002, Evaluation of 1D and 2D numerical models for predicting river flood inundation. Journal of Hydrology, 268: 87-99.

Hunter, N.M., Bates, P.D., Horritt, M.S. and Wilson, M.D., 2007, Simple spatially-distributed models for predicting flood inundation: A review. Geomorphology, 90: 208-225.

Merwade, V., Cook, A. and Coonrod, J., 2008, GIS techniques for creating river terrain models for hydrodynamic modeling and flood inundation mapping. Environmental Modelling and Software, 23: 1300-1311.

Merwade, V.M., Maidment, D.R. and Hodges, B.R., 2005, Geospatial Representation of River Channels. Journal of Hydrologic Engineering, 10: 243.

Merwade, V.M., Maidment, D.R. and Goff, J.A., 2006, Anisotropic considerations while interpolating river channel bathymetry. Journal of Hydrology, 331: 731-741.

Nunes Correia, F., Castro Rego, F., Da Graca Saraiva, M. and Ramos, I., 1998, Coupling GIS with Hydrologic and Hydraulic Flood Modelling. Water Resources Management, 12: 229-249.

Setegn, S.G., Srinivasan, R. and Dargahi, B., 2008, Hydrological Modelling in the Lake Tana Basin, Ethiopia Using SWAT Model. The Open Hydrology Journal, 2: 49-62.

SMEC, 2007, Hydrological Study of the Tana-Beles Sub-Basins. Draft Inception Report. Snowy Mountains Engineering Corporation, Australia.

Smith, L.C., 1997, Satellite Remote Sensing of River Inundation Area, Stage, and Discharge: A Review. Hydrological Processes, 11: 1427-1439.

Stelling, G.S. and Duinmeijer, S.P.A., 2003, A staggered conservative scheme for every Froude number in rapidly varied shallow water ows. International Journal for Numerical Methods in Fluids, 43: 1329-1354.

Stevens, N.F., Garbeil, H. and Mouginis-Mark, P.J., 2004, NASA EOS Terra ASTER: Volcanic topographic mapping and capability. Remote Sensing of Environment, 90: 405-414.

Swan, R., Howells, L., Bonello, D., Watkinson, R., Robertson, J., Treloar, C.L., Hawthorn, V.I.C. and Vic, E.M., 2007, Flood Studies and Extreme Events-Modelling,Mitigation and assessment at Fairfield,Victoria. 5th Victorian Flood Management Conference.

Tate, E.C., Maidment, D.R., Olivera, F. and Pe, D.J.A., 2002, Creating a Terrain Model for Floodplain Mapping. Journal of Hydrologic Engineering, 7: 100.

UNOCHA, 2006, Flood Affected Woredas in Ethiopia.http://www.ochaeth.org/Home/downloadables/FD_0014_RecentFlood_WWW.pdf.[Accessed in August 2008].

Werner, M., 2004, Spatial flood extent modelling: A performance-based Comparison, PhD Thesis, TU Delft, The Netherlands

Werner, M.G.F., 2001, Impact of grid size in GIS based flood extent mapping using a 1D flow model. Physics and Chemistry of the Earth, Part B, 26: 517-522.